Lt. Wm. Chas. F. Wilcarthy
Asst. Gen. Mgr.
Chance Vaught Aircraft

SPECIAL REPORT No. 93

INVESTIGATION IN THE 7- BY 10-FOOT WIND TUNNEL OF DUCTS FOR COOLING RADIATORS WITHIN AN AIRPLANE WING

By Thomas A. Harris and Isidore G. Recant
Langley Memorial Aeronautical Laboratory

July 1938

INVESTIGATION IN THE 7- BY 10-FOOT WIND TUNNEL OF DUCTS FOR COOLING RADIATORS WITHIN AN AIRPLANE WING

By Thomas A. Harris and Isidore G. Recant

SUMMARY

An investigation was made in the N.A.C.A. 7- by 10-foot wind tunnel of a large-chord wing model with a duct to house a simulated radiator suitable for a liquid-cooled engine. The duct was expanded to reduce the radiator losses, and the installation of the duct and radiator was made entirely within the wing to reduce form and interference drag. The tests were made using a two-dimensional-flow set-up with a full-span duct and radiator.

Section aerodynamic characteristics of the basic airfoil are given and also curves showing the characteristics of the various duct-radiator combinations. An expression for efficiency, the primary criterion of merit of any duct, and the effect of the several design parameters of the duct-radiator arrangement are discussed. The problem of throttling is considered and a discussion of the power required for cooling is included.

It was found that radiators could be mounted in the wing and efficiently pass enough air for cooling with duct outlets located at any point from 0.25c to 0.70c from the wing leading edge on the upper surface. The duct-inlet position was found to be critical and, for maximum efficiency, had to be at the stagnation point of the airfoil and to change with flight attitude. The flow could be efficiently throttled only by a simultaneous variation of duct inlet and outlet sizes and of inlet position. It was desirable to round both inlet and outlet lips. With certain arrangements of duct, the power required for cooling at high speed was a very low percentage of the engine power.

INTRODUCTION

Cooling and interference drag of the power-plant installation on many present-day airplanes with externally mounted radiators absorbs from 14 to 20 percent of the available power at high speed. The cooling drag of radiators can be materially reduced by mounting them in properly designed ducts (reference 1). Tests indicate that

interference drag is substantially decreased and a considerable saving in total cooling power is realized by building these ducts into the wing.

The energy loss in a ducted-radiator system built into a wing is comprised of the following components:

1. An external loss due to breaks in the wing surface at the inlet and the outlet of the duct.

2. An internal loss due to friction on the duct walls, rate of duct expansion, and obstructions.

3. An internal loss due to the radiator core.

4. A loss caused by the weight of the radiator and the duct.

The present investigation, which is part of a comprehensive study of radiators in wing ducts, is primarily concerned with the determination of the optimum inlet and outlet positions and sizes for minimum total cooling power; no attempt is made to separate and measure the individual losses. The investigation has also been confined to tests of a model representing a cold standard Army 9-inch-core Prestone radiator. The effects of duct inlet and outlet position, size, and shape were investigated with radiators of several heights located at two different positions within the wing. The data are sufficiently complete to permit the rational design of efficient duct and radiator combinations within the wing, although due consideration must be given to the fact that they were obtained from two-dimensional-flow tests and allowance must be made when they are applied to ducts of finite span.

APPARATUS AND TESTS

Airfoil

The basic model, or plain airfoil, tested has a chord of 3 feet and a span of 7 feet. The N.A.C.A. 23017 section was used because it is representative in thickness of wings in which radiators are likely to be installed and also because the results could be compared with results from tests of a wing of this section in the full-scale tunnel. The model (fig. 1) was built with solid nose and

trailing-edge pieces and has five solid ribs. The wing was covered with pressed-wood board to the required profile with an accuracy of ±0.015 inch. Openings could be made at practically any point on the upper or lower surface of the wing for taking in and discharging air and there was no internal structure to interfere with installation of the ducts.

Ducts

The ducts were built into the four compartments of the wing and were full span except for the ribs (fig. 1). The inlet and outlet of each duct were made of solid wood or metal; the top and the bottom of the duct to the radiator were of plywood or flat metal, the wing ribs forming the ends. The inlet and outlet positions of the ducts were selected from considerations of pressure distribution and location of the stagnation point at various angles of attack.

Duct designation.- The various ducts tested are designated by groups of four numbers to show the position and size of the inlet and outlet openings at the surface of the wing (figs. 2 to 7). The designations give approximately the position and size of the openings at the surface in percentage of wing chord. The exact positions and sizes of the various surface openings are shown in the sketches and tables.

The key to the designations is as follows:

inlet size - inlet position - outlet size - outlet position.

1. The first number in the group refers to the minimum size of inlet opening and is shown by the letter y in the sketches.

2. The second number refers to the position from the leading edge on the wing surface of the first break in the surface at the inlet. This distance is shown by the letter x for distances on the lower surface of the wing parallel to the chord line back of the leading edge, and by the letter x_a for distances perpendicular to and above the chord line; for this case the second number is followed by an appended a, as 1a, 2a, etc.

3. The third number gives the size of the outlet and is shown by the letter p on the sketches.

4. The fourth number refers to the first break in the upper surface of the wing at the duct outlet and is shown by the letter o on the sketches. Thus, a duct designated 6-1-8-70 has an inlet opening 6 percent of the wing chord with the first break in the surface 1 percent of the wing chord behimd the leading edge. The outlet opening is 8 percent of the wing chord and is located 70 percent of the wing chord behind the leading edge.

Duct combinations tested.- In figures 2 to 7 the upper sketch shows the various inlet shapes tested and the lower sketch is a sectional view of the duct showing the general arrangement; the table shows the proportions of the various duct combinations and arrangements tested. The positions and sizes of the inlet and the outlet openings are accurate to within $\pm 0.001c$.

Radiators

In the tests, the radiator (as has often been done heretofore) is simulated by a screen. The radiator chosen for representation was a standard Army 9-inch-core type made of 0.23-inch-diameter tubes with a 64.5-percent free-area ratio, f.

The screen used to represent the radiator is made in four sections of brass plate 1/4-inch thick with a suitable number of 1/4-inch holes so that the pressure drop for a given flow is the same as for the actual radiator. Tests of various screens showed that, for an approximate representation of the radiator, the screen should have a free-area ratio of about 42 percent.

A comparison of the characteristics of the radiator and of the screen is shown in figure 8. In this figure the pressure drop ΔP through the radiator or screen in terms of the dynamic pressure q_R at the face of the radiator or screen is plotted against the air velocity in the duct V_R. The radiator cannot be exactly represented at all velocities by this screen because of scale effect on the radiator; nevertheless figure 8 shows that, for the duct velocities encountered in the tests (30 to 40 miles per hour), the deviation of the screen from the radiator is small. This method of representation is therefore believed to be satisfactory; and, furthermore, there is close agreement between the amounts of air passing through the

screen and the radiator when they are installed in ducts outside the wing, the screen permitting 46 percent to pass and the radiator, 44 percent.

In order to measure the quantity of air passing through the duct without making detailed surveys for each arrangement, static-pressure and total-head tubes were built into one section of the radiator (the screen will be referred to hereinafter as a "radiator") as shown in figure 9. Calibration showed that such an arrangement was not very sensitive to air direction and that the quantity of air could be measured to within ±2 percent with duct arrangements similar to those used in the tests. The calibration also showed that the difference in pressure between the total-head and the static-pressure tubes was directly proportional to the dynamic pressure ahead of the radiator. The 24 pairs of the total-head and the static-pressure tubes were connected to a special multiple manometer for measurement during the tests of the dynamic pressure in three vertical and in eight horizontal planes in the holes of the radiator. The dynamic pressure ahead of the radiator was determined from the calibration constants. The radiator section with the measuring unit was mounted in one of the inboard wing compartments.

Radiators of different heights were obtained by altering the duct in such a way as to block off equal amounts on the top and the bottom of the radiator. (See fig. 3.)

Wind Tunnel and Balance

The N.A.C.A. 7- by 10-foot closed-throat wind tunnel and balance described in references 2 and 3 were used for making the tests.

Tests

The two-dimensional-flow installation described in reference 2 was used for the tests. The model completely spans the jet vertically in this installation and the results obtained are practically section characteristics.

A dynamic pressure of 16.37 pounds per square foot was maintained for all the tests and corresponds to an air velocity of about 80 miles per hour under standard sea-level atmospheric conditions and to an average test Reynolds Number of 2,190,000.

Tests were first made to obtain the characteristics of the plain wing for comparison with the various wing-duct combinations to be tested. The plain wing and the wing with the various duct arrangements were tested over the complete angle-of-attack range from zero to maximum lift. Data were obtained at 2° increments in angle of attack for all arrangements. Lift, drag, and pitching moment were measured for all combinations and, in addition, the quantity of air flowing through the radiator was measured for all arrangements with ducts.

RESULTS AND DISCUSSION

Coefficients

All aerodynamic characteristics of the wing with or without ducts are given in standard section nondimensional coefficient form, corrected as explained in reference 2.

α_o, section angle of attack.

c_l, section lift coefficient (l/qc).

c_{d_o}, section profile-drag coefficient (d_o/qc)

$c_{m_{a.c.}}$, section pitching-moment coefficient about aerodynamic center of plain wing $(m_{a.c.}/qc^2)$.

where

l is the section lift.

d_o, section drag.

$m_{a.c.}$, section pitching moment about aerodynamic center.

q, dynamic pressure $(\frac{1}{2} \rho V^2)$.

c, chord of wing.

In addition, the section characteristics of the duct are given in the following nondimensional form.

V_R/V, duct section flow ratio.

η, over-all duct section efficiency $(Q_o \Delta P/\Delta d_o V)$

where V_R is the air velocity in duct at face of radiator.

V, air velocity in free stream, or flight speed.

Q_o, quantity of air passing through duct per unit frontal area.

ΔP, pressure drop through radiator per unit frontal area.

Δd_o, increase in section profile drag caused by the duct at any given lift coefficient.

The flow ratio V_R/V is a measure of the quantity of air flowing through the radiator per unit frontal area. At a given flow ratio, the size of radiator required for a given installation may be determined, when the flight speed V and quantity of air Q are known, from the relationship $Q = AV_R$, or

$$A = \frac{Q}{\left(\frac{V_R}{V}\right) V} \qquad (1)$$

where A is the area of the radiator.

The efficiency η of a given installation is a criterion of the relative merit of the arrangement. The expression for efficiency was derived as follows:

$$\eta = \frac{\text{useful work}}{\text{total work}} = \frac{P_c}{P_T}$$

which is a basic efficiency formula. In this expression the useful work is considered to be the power expended in forcing the air through the radiator and the total work is the additional power required to pull the ducted wing through the air. Then

$$P_c = Q\Delta P = \Delta P A V_R = K\, q_R\, A\, V_R$$

and

$$P_T = \Delta d_o\, V = \Delta c_{d_o}\, q\, S\, V$$

where

$$K = \frac{\Delta P}{q_R} = 3.7$$

(see fig. 8) and other symbols have been previously defined.

Therefore, $$\eta = \frac{KA}{\Delta c_{d_o} S} \left(\frac{V_R}{V}\right)^3 \qquad (2)$$

where S is the area of the wing. The total power required for a given installation may then be obtained from the expression

$$P_T = \frac{KA\rho}{2\eta} \left(\frac{V_R}{V}\right)^3 V^3 \qquad (3)$$

where ρ is the mass density of the air.

Substituting the expression given by equation (1) for A, equation (3) becomes

$$P_T = \frac{1}{2} \rho V^2 KQ \frac{\left(\frac{V_R}{V}\right)^2}{\eta} \qquad (4)$$

or

$$P_T = \frac{KQ}{C_L} \frac{W}{S} \frac{\left(\frac{V_R}{V}\right)^2}{\eta} \qquad (5)$$

where $\frac{W}{S}$ is the wing loading of the airplane

For unit quantity and unit wing loading

$$P_T = \frac{3.7}{C_L} \frac{\left(\frac{V_R}{V}\right)^2}{\eta} \qquad (6)$$

so that at any given speed the power will be a minimum when the ratio $\frac{(V_R/V)^2}{\eta}$ is a minimum.

The expression for duct efficiency is not an absolute criterion of merit for the complete cooling installation. It is merely "pump efficiency" and is a measure of the duct loss in terms of the radiator loss. An efficiency of 1.0 (100 percent) indicates that the duct itself is not contributing to the increase in drag as measured or that favorable interference effects compensate for all losses except the loss through the radiator. Therefore, two duct-radiator

installations, each having the same efficiency, may not have the same merit; that is, one may absorb more power than the other. The detrrmining factor would then be the flow ratio, the one with the smaller flow ratio requiring less power. The total-power equation shows that the power is inversely proportional to the efficiency and directly proportional to the square of V_R/V, which indicates very large radiators. The final selection of radiator size will therefore be a compromise arrived at from considerations of the weight of the radiator installation.

Efficiencies greater than 1.0 can be explained by favorable interference effects that more than counterbalance the duct losses.

Precision

The accuracy of the various components measured in the force tests is:

α ..... $\pm 0.1^\circ$	c_{d_o} at $c_l = 0$ ..... ± 0.0003
$c_{l_{max}}$ ..... ± 0.03	c_{d_o} at $c_l = 1.0$ ... ± 0.0006
$c_{m_{a.c.}}$ ..... ± 0.003	c_{d_o} at $c_{l_{max}}$ ..... ± 0.0020

Although the error in the determination of the dynamic pressure in the duct q_R is no greater than 2 percent, the error in the flow ratio V_R/V may be much larger, as V_R has been determined from the average q_R obtained by a mechanical integration of the dynamic-pressure surveys at the radiator. This error is also present in the computation of efficiency. The magnitude of the error in the flow ratio, however, is an inverse function of the uniformity of the dynamic-pressure distribution across the face of the radiator. All duct arrangements with efficiencies above about 0.6 have a very nearly uniform dynamic-pressure distribution over the radiator, and the error in V_R caused by this method of computation is less than 2 percent for cases checked by integration of $\sqrt{q_R}$ distributions. For low efficiencies, V_R may be in error as much as 25 percent; the lower the efficiency, the greater the error. The low efficiencies are, in general, a result of burbled air flow on either the upper or the lower entrance lip,

which causes a large increase in drag and a nonuniform dynamic-pressure distribution at the radiator. Such arrangements are of no practical interest and it was considered that the additional work required to obtain V_R more accurately was not justified. The ratios of V_R/V and η (as affected by V_R) are believed to be accurate to within ±4 percent for all cases where η is greater than about 0.6. This procedure also assumed the flow to be symmetrical in the compartment in which it was measured and to be of the same value in the other three wing compartments. An additional error may be introduced into the efficiency by inaccuracy in drag measurement and the consequent error in the determination of Δc_{d_o}.

Plain Airfoil

The section aerodynamic characteristics of the plain N.A.C.A. 23017 airfoil, as determined from the two-dimensional-flow tests, are given in figure 10. There is some variation between these characteristics and those obtained from finite-span-model tests corrected to infinite aspect ratio. The slope of the lift curve, and the minimum profile-drag coefficient are slightly higher for the two-dimensional-flow set-up; the pitching-moment coefficients about the aerodynamic center are approximately equal. The chordwise location of the aerodynamic center is about the same in both cases, but its vertical distance above the chord is greater for the finite-span model. The degree of variation of the N.A.C.A. 23017 airfoil characteristics as obtained by each of the previously mentioned methods is about the same as the variations of the N.A.C.A. 23012 airfoil characteristics when obtained by finite-span and two-dimensional-flow tests. (See reference 2.)

Airfoil with Ducts

Dynamic-pressure distribution at radiator.- Figure 11 gives sample vertical and horizontal dynamic-pressure distributions at the face of the radiator at low and high angles of attack for two ducts, each having inlet radii of 0.005c, outlet radii of 0.08c, radiator heights of 0.14c, and radiator location of 0.20c behind the leading edge. Duct 8-1a-8-25 (fig. 7(a)), which is used for illustration of high angle-of-attack distribution, shows a fairly uniform vertical distribution (fig. 11(a)), although the dynam-

ic pressure falls off near the bottom of the duct, probably owing to flow separation over the lower lip. In the case of duct 5-4a-3-32 at 2° angle of attack, it can be seen from figure 7(b) that the inlet angle is not excessive and that the duct is fairly symmetrical about the center line of the tube of air entering it, so that the vertical distribution (fig. 11(a)) is therefore quite uniform. The horizontal distribution (fig. 11(b)) for both ducts is very regular. It is to be remarked that ducts which give fairly uniform distribution have reasonably high efficiencies. Conversely, poor distributions are associated with low efficiencies.

Effect of ducts on plain-wing characteristics.- In general, the ducts increase the drag, decrease the maximum lift, and shift the lift curve so as to give a lower lift at the same angle of attack than the plain wing. The drag increase is, of course, due to the breaks in the wing surface, to the radiator, to the friction of the duct walls, etc. The decrease in lift and the shift of the lift curve are probably due to the energy losses in the duct, which result in a decrease in circulation around the wing. In several instances where the outlet openings are small, causing high outlet speeds, the maximum lift does not drop off and sometimes surpasses the maximum lift of the plain wing.

Effect of inlet radii.- Figure 12 shows the effect of (a) lower lip and (b) upper lip inlet radii. The $c_{l_{max}}$ increases with an increase in the radius of either lip until a radius of 0.005c is reached. For this value of upper-lip radius, the $c_{l_{max}}$ is nearly the same as that of the plain wing. Further increase in the radius has either no effect or an unfavorable one.

The flow ratio, V_R/V, is practically unaffected by the radius of either lip at high speed (low lift coefficients) until a value of 0.005c is reached. Larger radii are unfavorable. At low-speed lift coefficients, V_R/V increases with an increase in lower-lip radius but is unaffected by the upper-lip radius.

At low speed (high lift coefficients) the efficiency η increases with an increase in the lower-lip radius, and is practically unaffected by upper-lip radii of 0.005c or below. At high speed (low lift coefficients) a radius

of either lip greater than 0.005c has an unfavorable effect on the efficiency. All subsequent tests were therefore made with both inlet radii of 0.005c.

Effect of outlet radius.- Figure 13 shows the effect of outlet radius (a) with the outlet at 0.70c, (b) with outlet at 0.45c, and (c) with outlet at 0.25c. It is interesting to note that the 0.08c radius gives the highest $c_{l_{max}}$ no matter which outlet position is chosen, but it is possible that this value holds only for the N.A.C.A. 23017 airfoil section. In all cases the flow ratio V_R/V decreases with a decrease in outlet radius. This effect is to be expected since the smaller the radius, the smaller the opening on the upper surface of the wing.

The efficiency at high-speed lift coefficients decreases with a decrease in the outlet radius for all outlet positions, although the degree of decrease varies with the outlet position. At low-speed lift coefficients the efficiency increases with a decrease in outlet radius within limits. This result is clearly shown at the 0.25c outlet position (fig. 13(c)), where at high lift coefficients the efficiency increases as the radius decreases from 0.20c to 0.08c. When the radius is decreased to zero, however, the efficiency is sharply reduced.

It is evident from figure 13(c) that a rounded outlet is desirable because of its favorable effects on η, V_R/V, and $c_{l_{max}}$. The best radius size is arrived at by compromise and varies with the outlet position. With outlet positions between 0.45c and 0.70c, a 0.25c radius gives the best results. As the outlet position moves forward from the 0.45c point, the radius should become smaller and, at the 0.25c position, an 0.08c radius is best.

Effect of radiator position.- Two radiator positions were investigated with the duct outlet at 0.70c; the results are shown in figure 14. The flow ratio and the efficiency are both decreased when the radiator position is moved ahead from 0.50c to 0.20c. This result, which was anticipated, is caused by the excessive duct inlet angle and consequent large duct losses when the radiator is in the forward position. It was necessary, however, to locate the radiator in the forward position in order to investigate outlet openings near the leading edge of the wing where larger pressure differences are available for forcing

air through the radiator. It will be shown later that high efficiencies and flow ratios may be obtained with the radiator in the forward position and with the outlet near the leading edge.

Effect of inlet position.- Figures 15 to 17 show the effect of inlet position. It can be seen from the figures that, whereas the $c_{l_{max}}$ is only slightly affected by variation of position from the leading edge to 0.02c behind the leading edge; movement of the position above the chord causes the $c_{l_{max}}$ to fall off, the magnitude of the loss varying with the distance above the chord. Positions 0.01c to 0.02c back of the leading edge markedly decrease the slope of the lift curve in the high-speed range.

The flow ratio increases as the inlet position moves forward and above the chord. This increase is most marked at the high-speed lift coefficients, probably owing to the fact that, for positions behind the leading edge and below the chord, the upper lip makes a large angle with the air flow and causes considerable burbling.

The efficiency increases considerably as the inlet position is moved forward and above the chord, particularly at low lift coefficients. This increase is probably due to the increase in the flow ratio, because the drag is increased as the position moves forward. Apparently, the flow increases much faster than does the drag. Thus, it is possible to obtain efficiencies from 0.85 to 1.0 for a lift coefficient range of 0.2 to 0.8 for any outlet position.

The results presented in figures 15 to 17 show quite clearly that it is impossible efficiently to throttle the flow by variation of inlet position alone. For example, figure 15(a) shows that approximately proper throttling from low-speed flow ratio to high-speed flow ratio may be obtained by varying the inlet position from 0.02c above the chord to 0.02c behind the leading edge as flight speed is increased. Under such conditions, the efficiency of the arrangement will drop from about 1.0 at low speeds to about 0.2 at high speeds with the consequent increase in power required.

Effect of outlet position.- Figure 18 shows the effect of outlet position (a) with the radiator at the 0.50c

point and (b) with the radiator at the 0.20c point. The $c_{l_{max}}$ decreases slightly as the outlet position is moved forward from the 0.70c point to the 0.45c point. Additional movement forward of the outlet causes a sharp decrease in $c_{l_{max}}$. The shape of the lift curve is markedly changed as the outlet position is moved forward. Also, there is a small unfavorable shift of the lift curve as the outlet is moved forward.

The flow ratio slightly increases as the outlet moves forward from 0.70c to 0.45c, but additional forward movement causes it to increase rapidly until, at the 0.25c point, it approaches 0.44 for a lift coefficient corresponding to climb. This value is about equal to the flow ratio of the radiator exposed in a free air stream so that, with the 0.25c outlet, it would be possible to use a radiator that would be no larger than those used in externally exposed installations.

The efficiency at low-speed lift coefficients is substantially reduced as the outlet position is moved forward, varying from 1.0 at the 0.70c outlet to 0.65 at the 0.25c outlet. At high-speed lift coefficients, however, the efficiency is practically unaffected as the outlet position is moved forward, provided that the proper inlet position is used.

Effect of inlet size.- The effects of duct inlet size with three heights of radiator are shown in figure 19 with the duct outlet at 0.70c. The $c_{l_{max}}$ decreases with decreasing inlet size but, with inlet and outlet size the same, the $c_{l_{max}}$ is about the same as for the plain wing with any of the radiator heights. Some boundary-layer control is obtained with the inlet opening slightly larger than the outlet (fig. 19(c)) and a slight gain in maximum lift is obtained over that of the plain wing. The shift in lift at a given angle is about the same in all cases.

The flow ratio decreases, as might be expected, with decrease in inlet size for all radiator heights. It is of interest to note that the maximum flow ratio obtained with any of these arrangements is about the same in spite of the fact that the relative size of surface openings to radiator height is much greater for the smallest radiator.

The efficiency, in general, decreases as the inlet size decreases if the inlet size is never larger than the outlet size. With the radiator height of 0.14c (fig. 19(a)), the efficiency decreases when the inlet size is increased from 0.06c to 0.08c over the flight range from climb to high speed. It is believed, however, that this decrease is a result of the poor entry shape of the upper lip with the 0.08c inlet size. The efficiency also decreases with decreasing height of radiator, which indicates that, for best results, the duct span at the wing surface should be as small as possible.

The results plotted in figure 19 show that the inlet opening should be about the same size as the outlet opening for best results and that the inlet area should be about 70 percent of the free area of the radiator when the radiator height is a maximum. The results also show that it is impossible to throttle the flow efficiently by variation of inlet size alone in a chordwise direction. It may be possible to throttle the flow efficiently by a variation of the inlet size in a spanwise direction, but this method of throttling could not be employed in these tests.

The effect of inlet size with the duct outlet at 0.45c is shown in figure 20. The effects of varying the inlet size with this outlet position are about the same as for the outlet at 0.70c. The flow ratio is slightly greater for this outlet position with the optimum sizes of inlet and outlet. The highest efficiency is obtained with the inlet and outlet opening about the same size but it is slightly less than with the outlet at 0.70c.

The effect of variation of inlet size with the outlet at 0.32c is shown in figure 21 for two outlet sizes and two inlet positions. If a flow ratio of 0.44 is available at climb, the ducts shown in figure 21(b) give about the required amount of flow for high speed and, at the same time, the lift curves are shifted only a small amount. An efficiency of about 0.90 with the proper flow ratio can be obtained with the duct inlet 0.04c above the chord but, with this inlet position, there is a large loss in maximum lift coefficient. Both the efficiency and the flow ratio increase with increase in inlet size at climb or low speed. The large loss in efficiency with the smallest inlet openings may be attributed to burbled air flow in the duct because of the angle at which the air enters the duct and the large expansion angle in the duct.

The effect of inlet size on the various parameters is about the same with the outlet at 0.28c (fig. 22) as with the outlet at 0.32c. The flow ratio is higher because of the larger outlet size. This outlet position is an intermediate position of an arrangement that was designed for throttling by movement of the upper outlet lip.

With the outlet at 0.25c (fig. 23), the variation of inlet size had about the same effect as for the other outlet positions. When the inlet is 0.01c above the chord (fig. 23(a)) and the outlet and inlet are the same size, the highest efficiencies are obtained at climb with a flow ratio of about 0.45. The large loss in maximum lift may be recovered by reducing the outlet size to that of the arrangement shown in figure 21(a). A further discussion of throttling this arrangement will be given later. With the inlet 0.04c above the chord (fig. 23(b)), the results are not of much interest because of the large flow ratio at high speed, the drop in efficiency at climb, and the large loss in maximum lift coefficient.

Effect of outlet size.- The effect of a variation in the outlet size with the outlet at 0.70c (fig. 24) is typical of the effect with the outlet at the other locations. From these results it may be seen that, regardless of radiator height, the lift curve is shifted favorably as the outlet size is decreased. Furthermore, when the outlet size is small compared with the inlet size, boundary-layer control is obtained and the maximum lift coefficient is markedly increased over that of the plain airfoil. The flow ratio, as might be expected, decreases with decreasing outlet size. In every case, however, when the outlet size is decreased to throttle the flow at high speed, the efficiency is greatly reduced although the power required for cooling may be decreased. The arrangement with the entrance 0.02c above the chord line (fig. 24(c)) does, however, give an efficiency of over 0.80 when approximately throttled for high speed by a variation of only outlet size. This result is not obtained in climb, where some boundary-layer control is obtained and the efficiency is increased as the outlet size is decreased for the 0.14c radiator. (See fig. 24(a), (b), and (c).) A comparison of figures 21 to 23 shows the same results with the outlet located between 0.25c and 0.32c (arrangements that were designed for throttling) as with the 0.70c outlet position.

Application of Data

Selection of duct for throttling.- For automatic throttling of a given duct arrangement, it is necessary that V_R be the same for all speeds or that the flow ratio be proportional to the square root of c_l, i.e.,

$$\frac{V_R}{V} = K_1 \sqrt{c_l} \tag{7}$$

Practically none of the arrangements satisfy this condition, the flow usually being too high at low lift coefficients. Whenever a particular duct gives a flow ratio approximately following this law, the efficiency is very small at high speed. It is therefore necessary to use some mechanical means of throttling the flow while maintaining a high efficiency at high speed. It has already been shown that efficient throttling at this speed probably cannot be obtained by decreasing chordwise inlet or outlet size alone. An analysis of the test results shows that it is possible efficiently to throttle the flow by a simultaneous variation of the inlet and outlet sizes and also by a variation of the inlet position. The flow ratio at climb probably determines the size of radiator necessary for cooling and, if it is desired that the radiator in the duct be no larger than one fully exposed to the air, this ratio should be about 0.44. Duct 8-1a-8-25 (fig. 23(a)) has a flow ratio of 0.45 and an efficiency of 0.84 at $c_l = 0.7$, an assumed lift coefficient for climb. This duct arrangement shifts the angle of attack for the given lift about 4° but, since the duct width will probably be small, it is believed that the change in the induced drag will not be large. This additional drag may be computed.

It has been assumed, for illustration, that high speed will occur at $c_l = 0.25$. Now from equation (7) the flow ratio at high speed for satisfactory cooling should be 0.27. Duct 5-4a-3-32 (fig. 21(b)) gives nearly the correct flow ratio with an efficiency of 0.92 at high speed. The shift in the angle of attack for $c_l = 0.25$ is only about 1/2° and, therefore, the additional interference drag should be negligible. In order to obtain an arrangement with exactly the correct flow ratio and the highest efficiency, it is necessary to cross-plot (from figs. 21(b), 22(b), and 23(b)) the flow ratio and the efficiency against outlet size. (The actual outlet size should be used in this plot.) This method has been used for $c_l = 0.25$ and the result

is shown in figure 25(a). From figure 25(a) the efficiency for a flow ratio of 0.27 has been plotted against inlet size with the outlet size indicated on the plot, as shown in figure 25(b). The optimum arrangement with the flow ratio of 0.27 has an inlet opening of 0.052c and an outlet opening of 0.040c, which gives an efficiency of about 0.93. The cooling power required for this duct with the flow throttled will therefore be about 10 percent less at high speed than at climb since, for a given installation properly throttled for all speeds, the cooling power varies inversely as the efficiency. Such a method of throttling would be practicable in a design having the upper and the lower inlet lips and the upper outlet lip adjustable. In order to recover the section lift for landing, the inlet opening should be set for climb and the outlet opening for high speed.

None of the data presented herein show whether it will be possible to obtain cooling on the ground but it is probable that, with an arrangement having adjustable sizes of inlet and outlet and variable inlet position, cooling may be obtained on the ground if the duct is located in the propeller slipstream.

Power required for cooling.- The power required for cooling has been given by equation (3)

$$P_T = \frac{KA\rho}{2\eta}\left(\frac{V_R}{V}\right)^3 V^3$$

This equation may be rewritten in terms of horsepower and gives, when the value of $K = 3.7$ is substituted,

$$hp_T = \frac{1.85\ A\rho}{550\ \eta}\left(\frac{V_R}{V}\right)^3 V^3 \qquad (7)$$

where V is in feet per second and A is in square feet. If, for duct arrangement 8-1a-8-25 (fig. 23(a)), it is assumed that the flight speed is 170 feet per second at climb and that the quantity of air required to cool a 1,000-horsepower engine with Prestone cooling is 283 cubic feet per second, then from equation (1)

$$A = \frac{Q}{\left(\frac{V_R}{V}\right)V} = \frac{283}{0.45 \times 170} = 3.7 \text{ square feet}$$

$V_R/V = 0.45$ at $c_l = 0.7$ from figure 23(a). Also from this figure, η is equal to 0.84 at $c_l = 0.70$. The total horsepower required for cooling, neglecting secondary interference effects and radiator weight, will be:

$$hp_T = \frac{(1.85)\ (0.002378)\ (3.7)\ (0.45)^3\ (170)^3}{0.84 \times 550} = 15.8 \text{ hp.}$$

This arrangement has a radiator of about the same size as a conventional arrangement and is believed to use about 1.5 percent of the engine power for cooling at climb. At high speed, if throttled as indicated in the previous section, the total horsepower required will be

$$hp_T = \frac{0.84}{0.93}\ 15.8 = 14.3 \text{ horsepower}$$

or only 1.5 percent of the engine power as compared with present liquid-cooled installations that use from 14 to 20 percent of the engine power for cooling.

Equation (6) shows that the total cooling power is proportional to the ratio $\frac{(V_R/V)^2}{\eta}$. Hence, it is possible for the efficiency η to be quite low without any increase in cooling power if there is a corresponding decrease in the flow ratio V_R/V. The following table compares some of the better duct-radiator combinations on a power basis at climb and at high speed for unit quantity of air and wing loading.

When the table (p. 20) is used it must be kept in mind that, although some combinations with small efficiencies require low power for cooling, the small flow ratios which make such a condition possible necessitate larger radiator frontal areas and, consequently, greater radiator weights. It will probably be necessary to compute the effect of added weight for each individual installation, and a complete analysis of the problem is desirable. Treatments of the effect of radiator weight may be found in references 1 and 4.

TABLE I

POWER COEFFICIENTS OF DUCT-RADIATOR COMBINATIONS

Combination				Efficiency η		Flow ratio V_R/V		Power coefficient $\frac{3.7}{c_l}\frac{(V_R/V)^2}{\eta}$	
Designation	Radiator position (percent c)	Radiator height (percent c)	Outlet radius (percent c)	$c_l=0.7$	$c_l=0.25$	$c_l=0.7$	$c_l=0.25$	$c_l=0.7$	$c_l=0.25$
6-2a-8-70	50	14	25	0.79	1.04	0.357	0.352	0.85	1.76
6-2a-6-70	50	14	25	.96	1.00	.325	.305	.58	1.38
6-2a-4-70	50	14	25	1.16	.86	.264	.245	.32	1.03
6-2a-2-70	50	14	25	.43	.22	.150	.140	.28	1.32
6-0-8-70	50	14	25	1.00	.64	.374	.315	.74	2.29
6-0-6-70	50	14	25	1.11	.45	.329	.250	.52	2.06
6-0-4-70	50	14	25	1.16	.31	.260	.207	.31	2.05
6-0-6-70	50	10	25	.90	.48	.365	.292	.78	2.63
6-0-4-70	50	10	25	.85	.32	.300	.230	.56	2.45
6-0-2-70	50	10	25	.58	.09	.190	.134	.33	2.95
8-1a-8-25	20	14	8	.84	.48	.450	.345	1.27	3.67
8-1a-6-32	20	14	20	.91	.44	.394	.307	.90	3.17
8-1a-4-32	20	14	20	.94	.29	.300	.233	.51	2.77
8-2a-8-25	20	14	8	.89	.78	.426	.380	1.08	2.74
6-4a-3-32	20	14	8	.81	.74	.273	.235	.49	1.10
5-4a-3-32	20	14	8	.46	.92	.272	.242	.85	.94
4-4a-3-32	20	14	8	.15	.73	.234	.250	1.93	1.27

CONCLUSIONS

The results of the tests reported herein showed that:

1. The power required for cooling was only the power required to force air through the radiator for optimum duct-radiator arrangements within the wing.

2. The duct inlet position for maximum efficiency was dependent upon the angle of attack.

3. Maximum efficiencies were obtained when the stagnation point on the airfoil was at the duct-inlet opening.

4. The quantity of air could be efficiently throttled by a simultaneous variation of duct inlet and outlet size and of inlet position.

5. High efficiencies could be obtained with the outlet at any position on the upper surface of the wing from 25 to 70 percent from the leading edge.

6. Radii were desirable on both the upper and lower inlet lips and on the lower outlet lip.

7. For maximum efficiencies, the spanwise duct openings should be as short as possible.

8. The best efficiencies were obtained with the duct inlet and outlet approximately the same size, neglecting the expansion of air due to a hot radiator.

9. The computed power required for cooling with a good duct-radiator combination for any flight condition was less than 2 percent of the engine power.

Langley Memorial Aeronautical Laboratory,
National Advisory Committee for Aeronautics,
Langley Field, Va., June 9, 1938.

REFERENCES

1. Worth, Weldon: Bigger and Better Radiators. Aviation, vol. 34, no. 8, Aug. 1935, pp. 19-21.

2. Wenzinger, Carl J., and Harris, Thomas A.: Tests of an N.A.C.A. 23012 Airfoil with Various Arrangements of Slotted Flaps in the Closed-Throat 7- by 10-Foot Wind Tunnel. T.R. No. (to be published), N.A.C.A., 1938.

3. Harris, Thomas A.: The 7 by 10 Foot Wind Tunnel of the National Advisory Committee for Aeronautics. T.R. No. 412, N.A.C.A., 1931.

4. Hartshorn, A. S.: Note on Performance Data for Honeycomb Radiators in a Duct. R. & M. No. 1740, British A.R.C., 1936.

FIGURE LEGENDS

Figure 1.- Diagram of plain wing.

Figure 2.- Duct arrangements with various inlet radii.

Figure 3.- Duct arrangements with various radiator heights.

Figure 4.- Duct arrangements with various outlet sizes.

Figure 5.- Duct arrangements with outlet at 0.70c and radiator at 0.20c.

Figure 6.- Duct arrangements with outlet at 0.45c.

Figure 7.- Duct arrangements with outlets from 0.25c to 0.32c.

Figure 8.- Comparison of screen and radiator pressure drop.

Figure 9.- Pressure-tube locations on screen.

Figure 10.- Section aerodynamic characteristics of N.A.C.A. 23017 airfoil.

Figure 11.- Dynamic-pressure distribution at radiator for ducts 8-1a-8-25 and 5-4a-3-32. Entrance radii, 0.005c; exit radius, 0.08c; radiator height, 0.14c; radiator location, 0.20c.
(a) Vertical distribution.
(b) Horizontal distribution.

Figure 12.- Effect of inlet radii.
(a) Lower lip.
(b) Upper lip.

Figure 13.- Effect of outlet radius.
(a) Outlet at 0.70c.
(b) Outlet at 0.45c.
(c) Outlet at 0.25c.

Figure 14.- Effect of radiator position.

Figure 15.- Effect of inlet position with outlet at 0.70c.
(a) Inlet size, 0.06c.
(b) Inlet size, 0.08c.

Figure 16.- Effect of inlet position with outlet at 0.45c.

Figure 17.- Effect of inlet position.
(a) Outlet at 0.25c.
(b) Outlet at 0.28c.
(c) Outlet at 0.32c.

Figure 18.- Effect of outlet position.
(a) Radiator at 0.50c.
(b) Radiator at 0.20c.

Figure 19.- Effect of inlet size with outlet at 0.70c.
(a) Radiator 0.14c high.
(b) Radiator 0.10c high.
(c) Radiator 0.06c high.

Figure 20.- Effect of inlet size with outlet at 0.45c.

Figure 21.- Effect of inlet size with outlet at 0.32c.
(a) Inlet position 0.01c above chord.
(b) Inlet position 0.04c above chord.

Figure 22.- Effect of inlet size with outlet at 0.28c.
(a) Inlet position 0.01c above chord.
(b) Inlet position 0.04c above chord.

Figure 23.- Effect of inlet size with outlet at 0.25c.
(a) Inlet position 0.01c above chord.
(b) Inlet position 0.04c above chord.

Figure 24.- Effect of outlet size with outlet at 0.70c.
(a) Radiator 0.14c high.
(b) Inlet position 0.01c above chord.
(c) Inlet position 0.02c above chord.
(d) Radiator 0.01c high.

Figure 25.- Duct inlet and outlet sizes for throttling.
(a) Selection of η for V_R/V. c_l, 0.25.
(b) Optimum size of openings c_l, 0.25; V_R/V, 0.27.

[All dimensions are in percent c.]

Designation	Inlet $r_1 = r_2 = 0.5$				Outlet			Radiator	
	Piece								
	Upper	Lower	x_a	y	o	p	r_3	n	h
8-4a-8-70	12	8	4	8.2	70	8	25	50	14
8-1a-8-70	10		1	8					
7-2a-8-70	11		2	7					
8-0-8-70	9		0	8			8		
							4		
6-1a-8-70	13		1	6.3		6	25		
6-1a-6-70						4			
6-1a-4-70						2			
6-1a-2-70						0			
6-1a-0-70						2			
6-2a-0-70	11	10	2	5.8		4			
6-2a-2-70						6			
6-2a-4-70						8			
6-2a-6-70									
6-2a-8-70									

Table to accompany figure 4.

[All dimensions are in percent c.]

Designation	Inlet $r_1 = r_3 = 0.5$				Outlet			Radiator	
	Piece		x	y	o	p	r_3	n	h
	Upper	Lower							
6-0-8-70	28	18	0	5.73	70	8	25	20	14
8-0-8-70		28		7.81					

Table to accompany figure 5.

[All dimensions are in percent c.]

Designation	Inlet $r_1 = r_3 = 0.5$					Outlet			Radiator	
	Piece		x	x_a	y	o	p	r_3	n	h
	Upper	Lower								
6-2-8-70	5	8	2	-	6	70	8	25	50	14
6-0-8-70	3		0	0	4					
4-0-8-70		10			2					
2-0-8-70		7			4		6			
2-0-6-70		10			6					
4-0-6-70		8			4		4			
6-0-6-70		10			2					
6-0-4-70		7			6		8			
4-0-4-70	6	8	1	-	6	60				
2-0-4-70	7		-	1						
6-1-8-70	8		-	2						
6-1a-8-70	3	10	0	0	4	70	2	25	50	10
6-2a-8-70		7			2					
6-0-8-60		10			4		4			
6-0-2-70		8			6					
4-0-2-70		10			4		6			
2-0-2-70		7			2					
2-0-4-70		10			4		2			
4-0-4-70		8			6					
6-0-4-70		10			4		4		50	6
6-0-6-70		7			2					
4-0-6-70		8			6		6			
2-0-6-70		10			4					
		7			2					

Table to accompany figure 3.

[All dimensions are in percent c.]

Designation	Inlet							Outlet			Radiator	
	Piece				Radius							
	Upper	Lower	r_1	r_2	x	y	r_3	o	p	r_3	n	h
4-0-6-70	1	1	0	0	0	4	25	70	6	25	50	14
	1	2	0	.25								
	1	3	0	.5								
	1	4	0	1.0								
	1	5	0	1.5								
	2	5	.25	1.5								
	3	5	.5	1.5								
	4	6	1.0	2.0								
	3	5	.5	1.5								

Table to accompany figure 2.

[All dimensions are in percent c.]

Designation	Inlet $r_1 = r_2 = 0.5$ Piece Upper	Piece Lower	x	x_a	y	Outlet o	p	r_3	Radiator n	h
8-0-8-25	2S	2S	0	0	7.81	25	8	20	20	14
6-0-8-25		1S			5.73					
8-1-8-25	3S	2S	1	-	7.46					
6-1-8-25		1S			5.26					
6-2-8-25	4S	2S	2	-	5.8					
8-2-8-25		3S			7.8					
6-5-8-25	5S	3S	5	-	5.9					
8-5-8-25		4S			8					
6-1a-8-25	1S	1S	-	1	6.25					
6-1a-6-28	1S	1S	-	1	6.25	28	6			
8-1a-6-28		2S			8					
10-1a-6-28		3S			9.7					
10-2a-6-28	6S			2						
12-1a-6-28	1S	4S		1	11.5					
12-1-6-28	3S		1	-	11.2					
8-1a-4-32	1S	2S	-	1	8	32	4			
6-1a-4-32		1S			6.25					
6-2a-4-32	6S			2	6.8					
6-4a-4-32	7S			4	6.7					
8-2a-8-25	6S	2S	-	2	8.3	25	8	8		
8-4a-8-25	7S			4						
10-1a-8-25	1S	3S		1	9.7					
10-2a-8-25	6S			2						
10-4a-8-25	7S			4						
12-1a-8-25	1S	4S		1	11.3					
12-2a-8-25	6S			2						
12-4a-8-25	7S			4						
8-1a-8-25	1S	1S	-	1	8			20		
								8		
8-0-8-25	2S	2S	0	0	7.81			0		
6-4a-3-32	7S	1S	-	4	6.7	32	2.9	8		
6-4a-6-28						28	5.5			
8-4a-6-28		2S			8.3					

[All dimensions are given in percent c.]

Table to accompany figure 7a.

[All dimensions are in percent c.]

Designation	Inlet $r_1 = r_2 = 0.5$ Piece Upper	Piece Lower	x	x_a	y	Outlet o	p	r_3	Radiator n	h
6-1a-8-45	1S	1S	-	1	6.25	45	7.5	25	20	14
8-1a-8-45	1S	2S	-	1	8					
8-1-8-45	3S	2S	1	-	7.46					
6-1-8-45	3S	1S	1	-	5.21					
6-2-8-45	4S	2S	2	-	5.8					
8-2-8-45	4S	3S	2	-	7.8					
6-5-8-45	5S	3S	5	-	5.9					
8-5-8-45	5S	4S	5	-	8					
6-5-8-45	5S	3S	5	-	5.9		6			
6-2-6-45	4S	2S	2	-	5.8					
5-2-6-45	4S	1S	2	-	5.16					
6-1-6-45	3S	1S	1	-	5.21					
6-1a-6-45	1S	1S	-	1	6.25					
6-0-6-45	2S	1S	0	0	5.73					
8-1a-6-45	1S	2S	-	1	8					
8-1a-8-45	1S	2S	-	1	8		7.5	8		
10-1a-8-45	1S	3S	-	1	9.7					
10-1-8-45	3S	3S	1	-	9.7					
8-2a-8-45	6S	2S	-	2	8.3					
8-1-8-45	3S	2S	1	-	7.46					
8-4a-8-45	7S	2S	-	4	8.1					
6-0-8-45	2S	1S	0	0	5.73			25		
								15		
								8		
8-0-8-45	2S	2S			7.81			25		
								15		
								8		

Table to accompany figure 8.

Designation	Inlet $r_1 = r_2 = 0.5$ Piece Upper	Piece Lower	x_a	y	Outlet o	p	r_3	Radiator n	h
3-4a-8-25	7S	5S	4	3	25	8	8	20	14
4-4a-8-25		6S		4					
5-4a-8-25		7S		5					
4-4a-6-28		6S		4	28	5.5			
5-4a-6-28		7S		5					
3-4a-6-28		5S		3					
4-4a-3-32		6S		4	32	2.9			
5-4a-3-32		7S		5					

Table to accompany figure 7b.

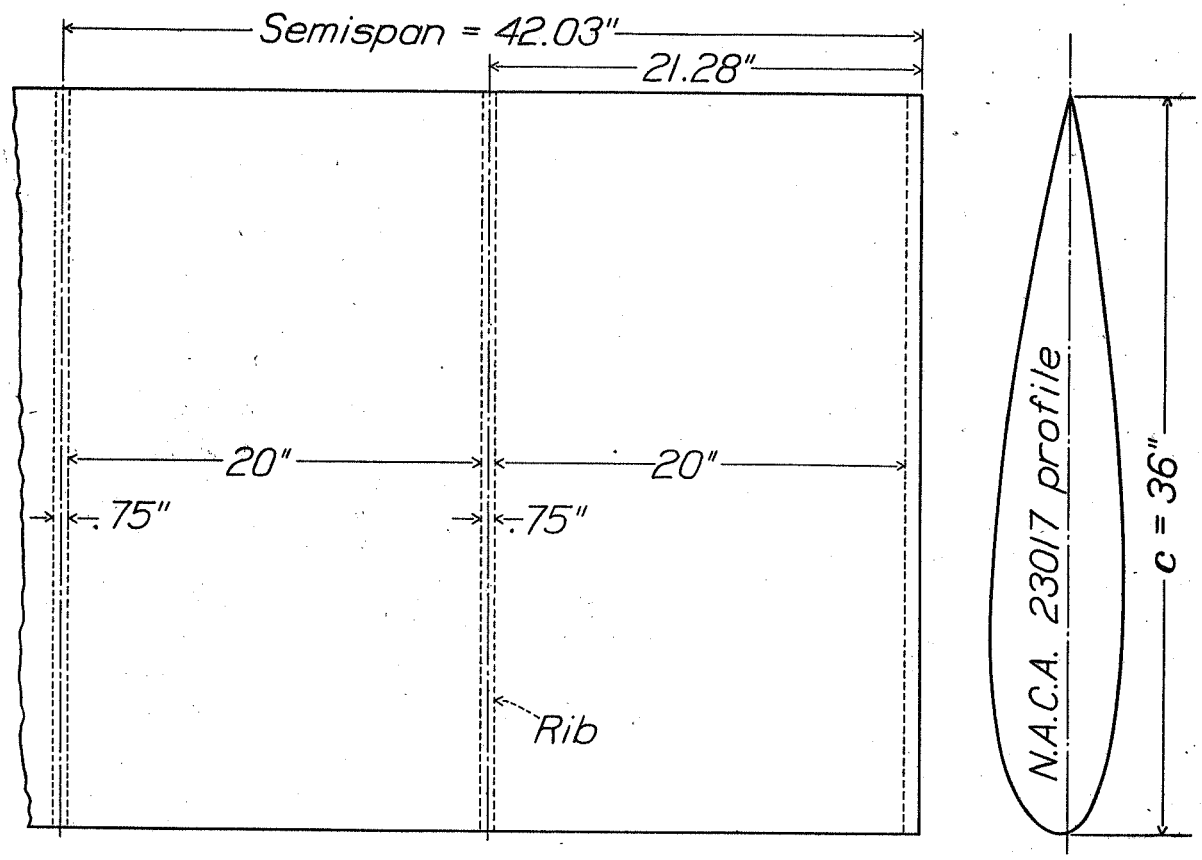

Figure 1

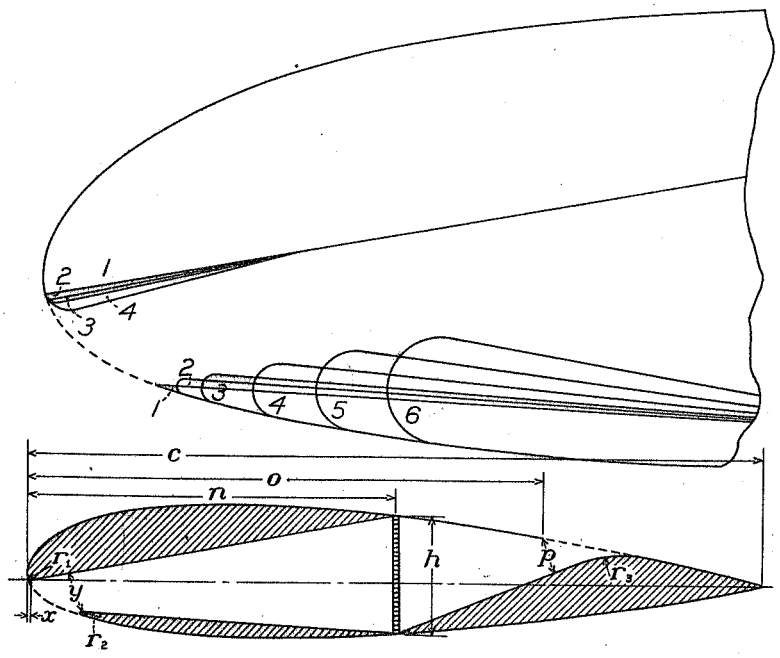

Figure 2

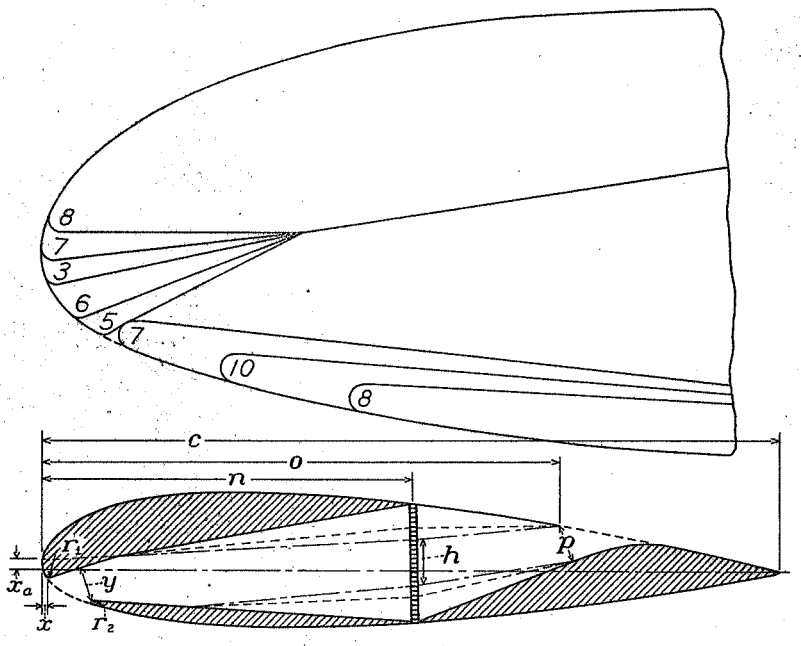

Figure 3

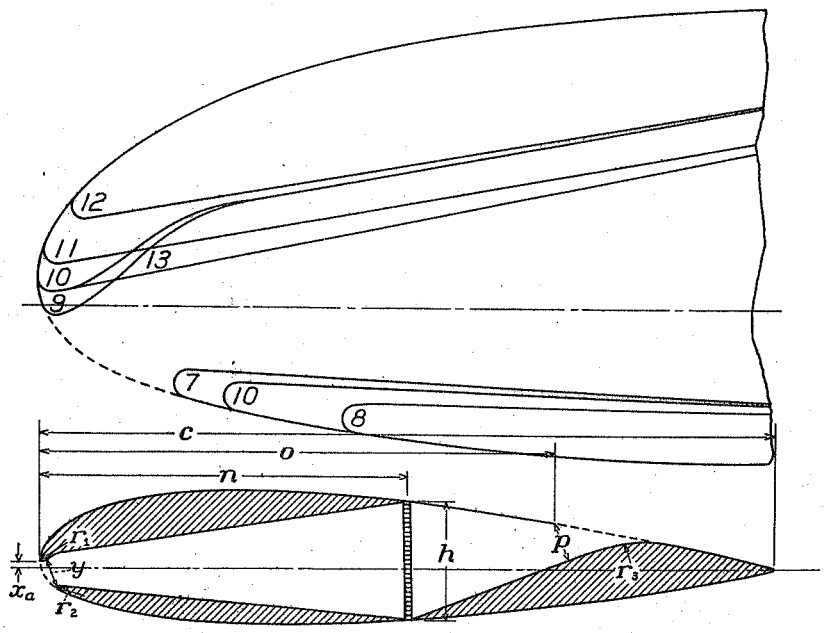

Figure 4

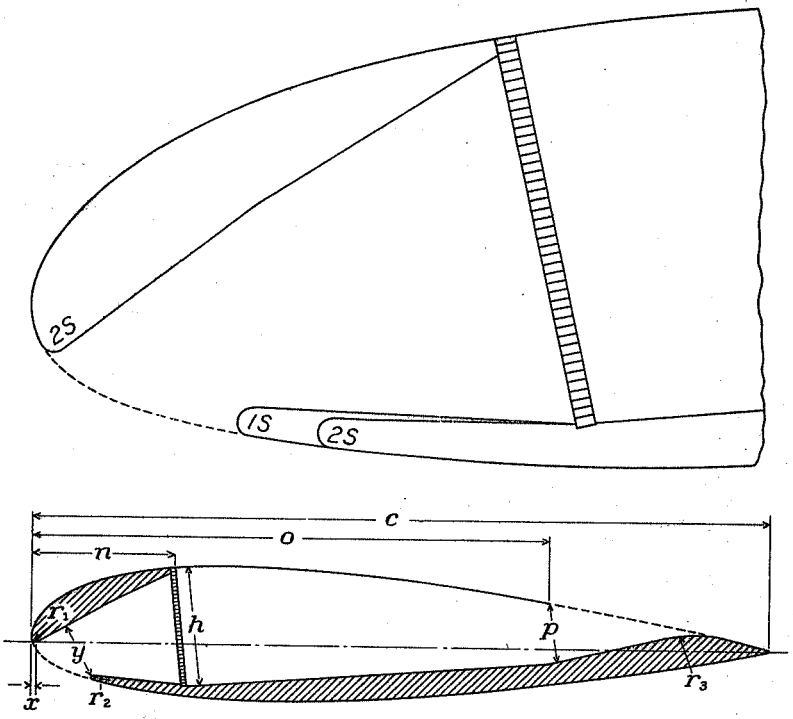

Figure 5

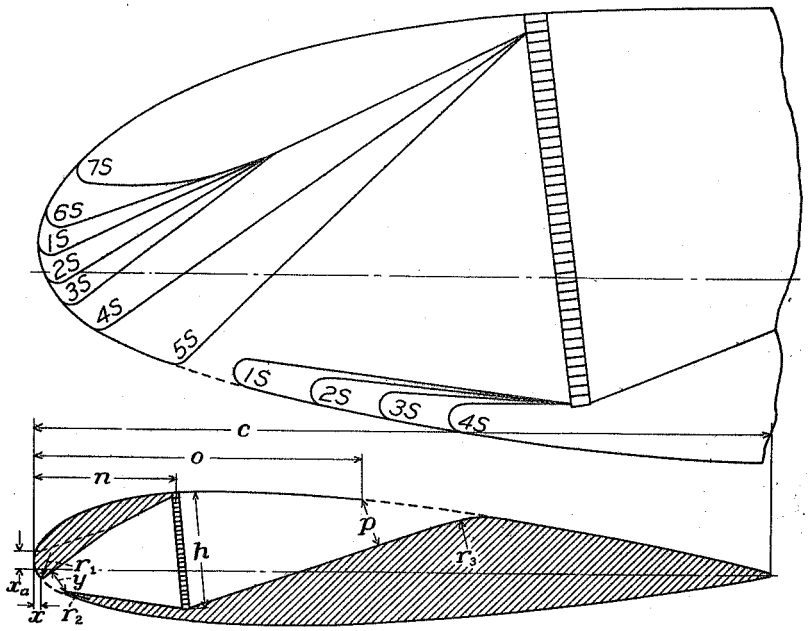

Figure 6

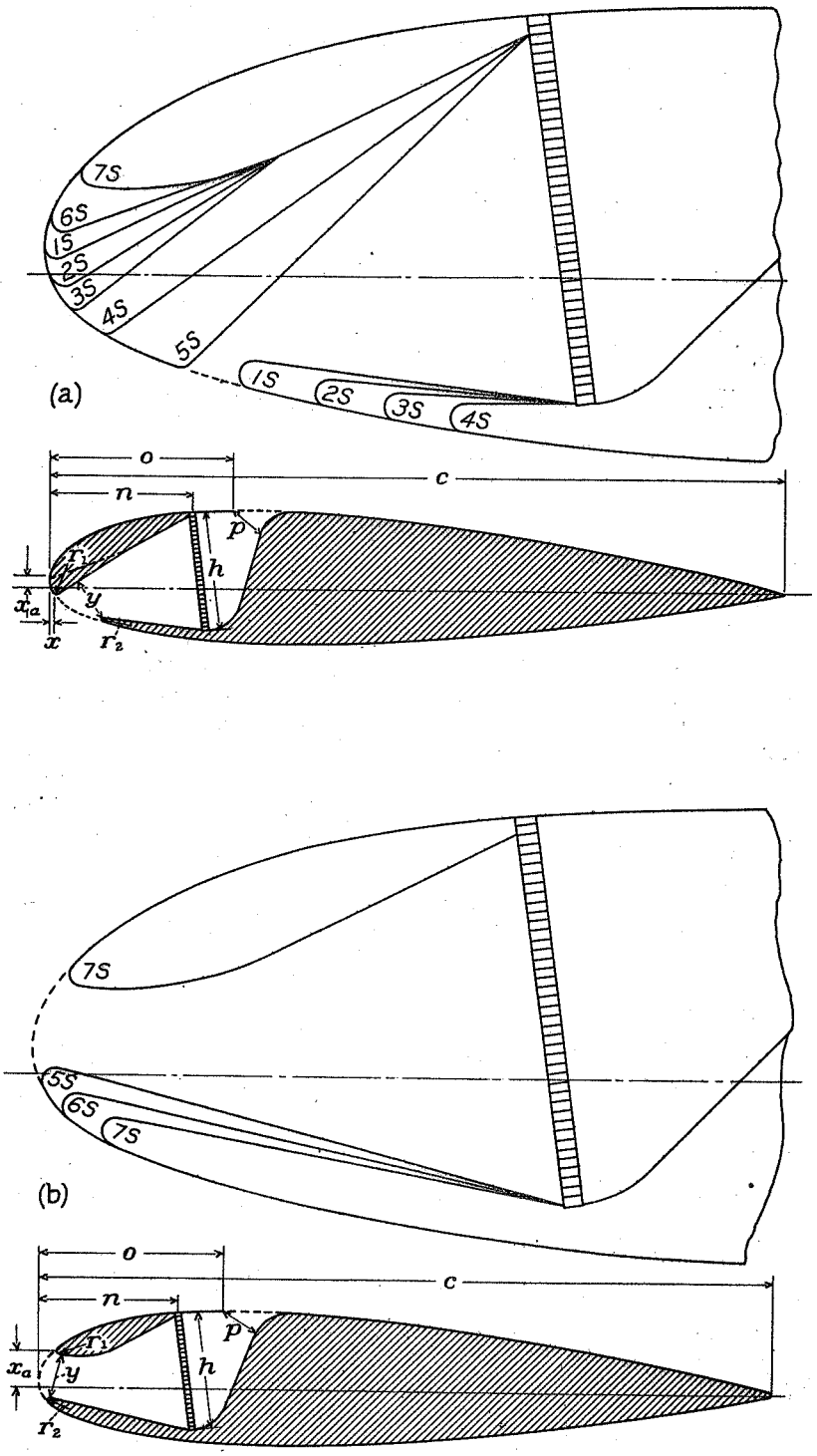
7S
6S
1S
2S
3S
4S
5S
1S
2S
3S
4S
(a)
o
c
n
p
h
r_1
y
x_a
x
r_2
7S
5S
6S
7S
(b)
o
c
n
p
r_1
x_a
y
h
r_2

Figure 7a,b.

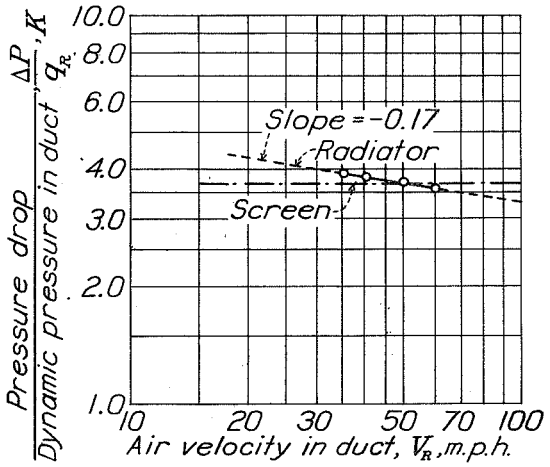

Figure 8

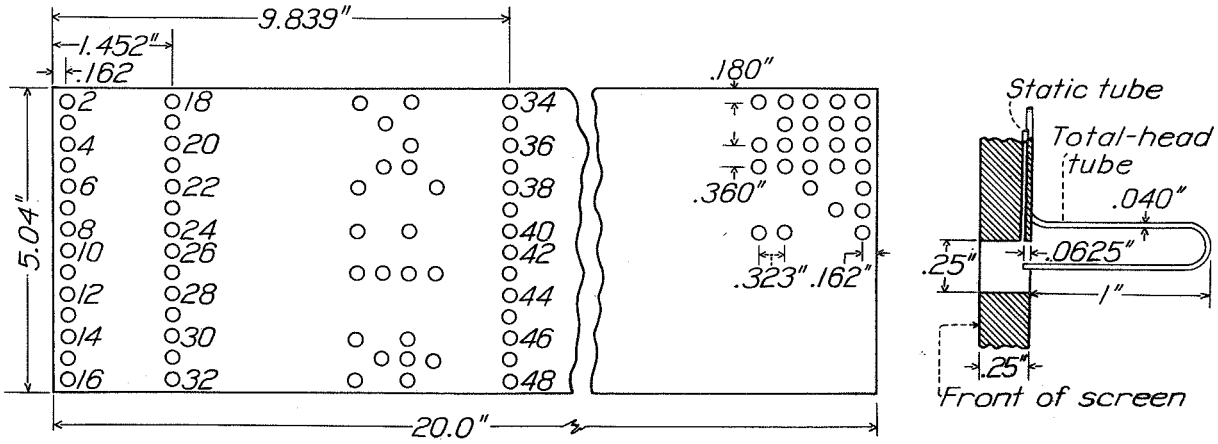

Figure 9

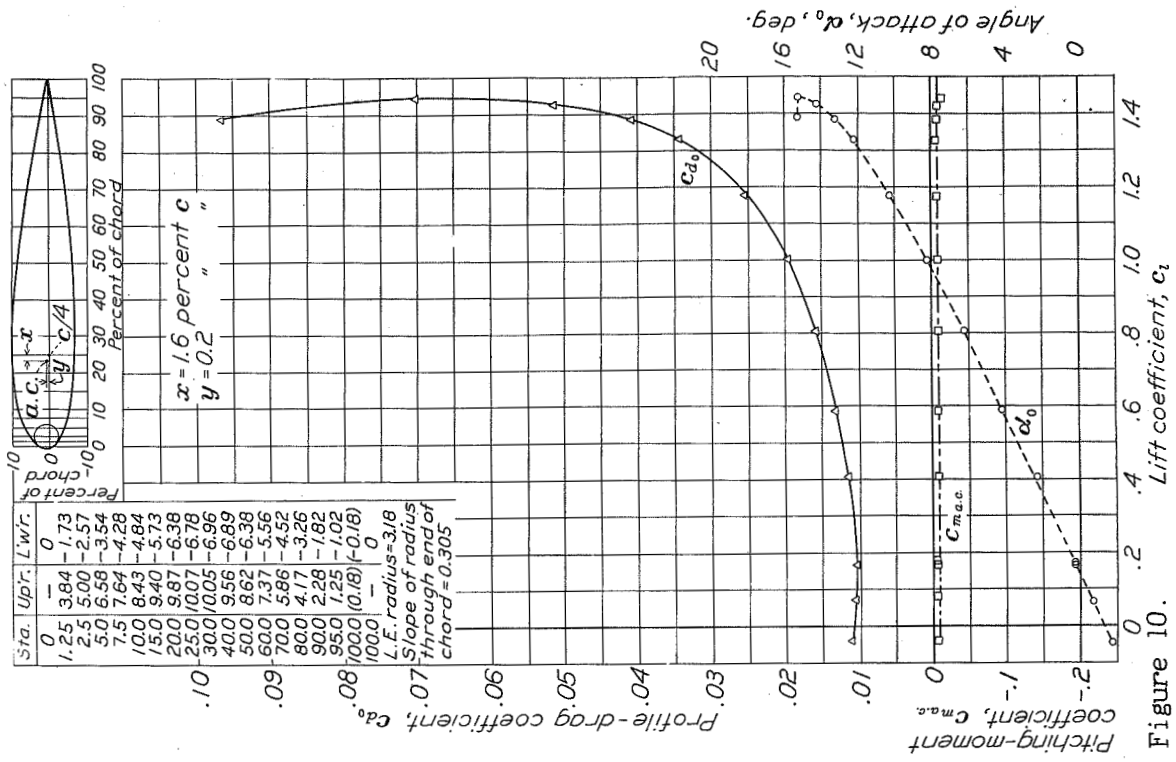

Figure 10.

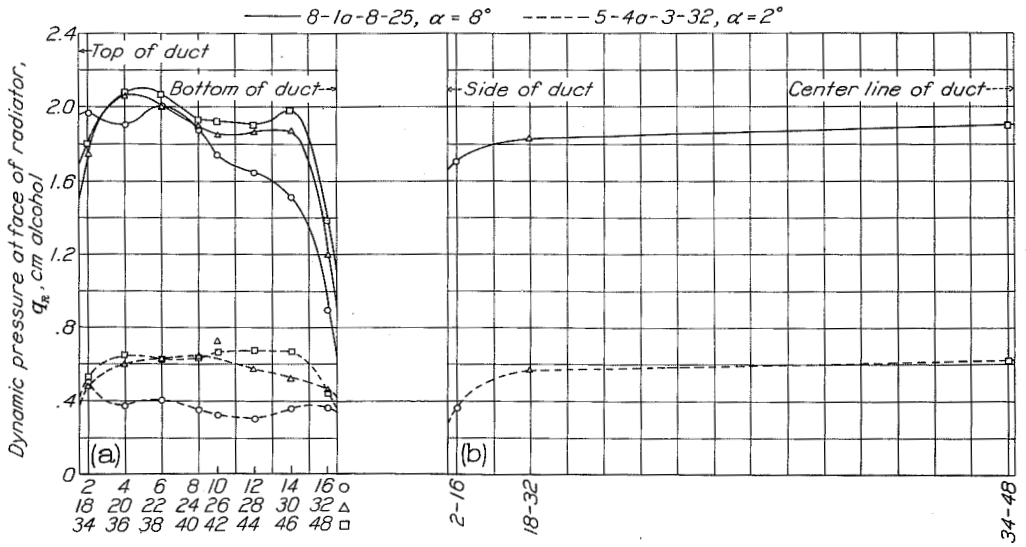

Figure 11 a,b.

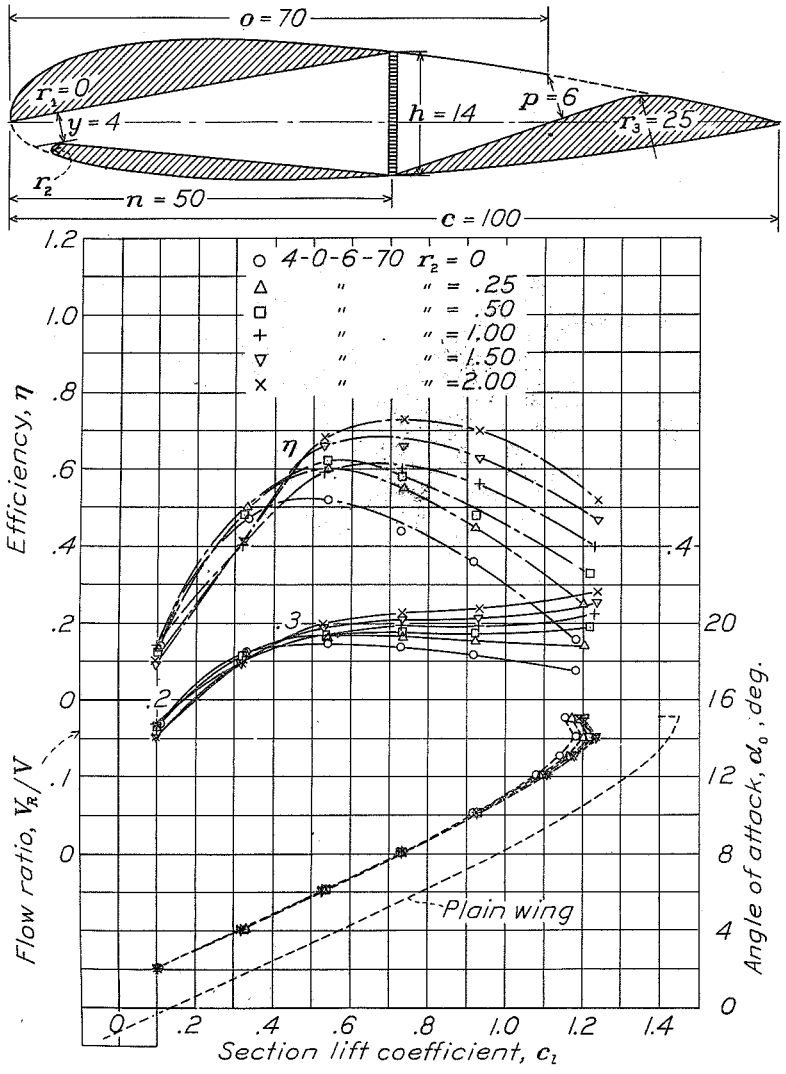

Figure 12 a.

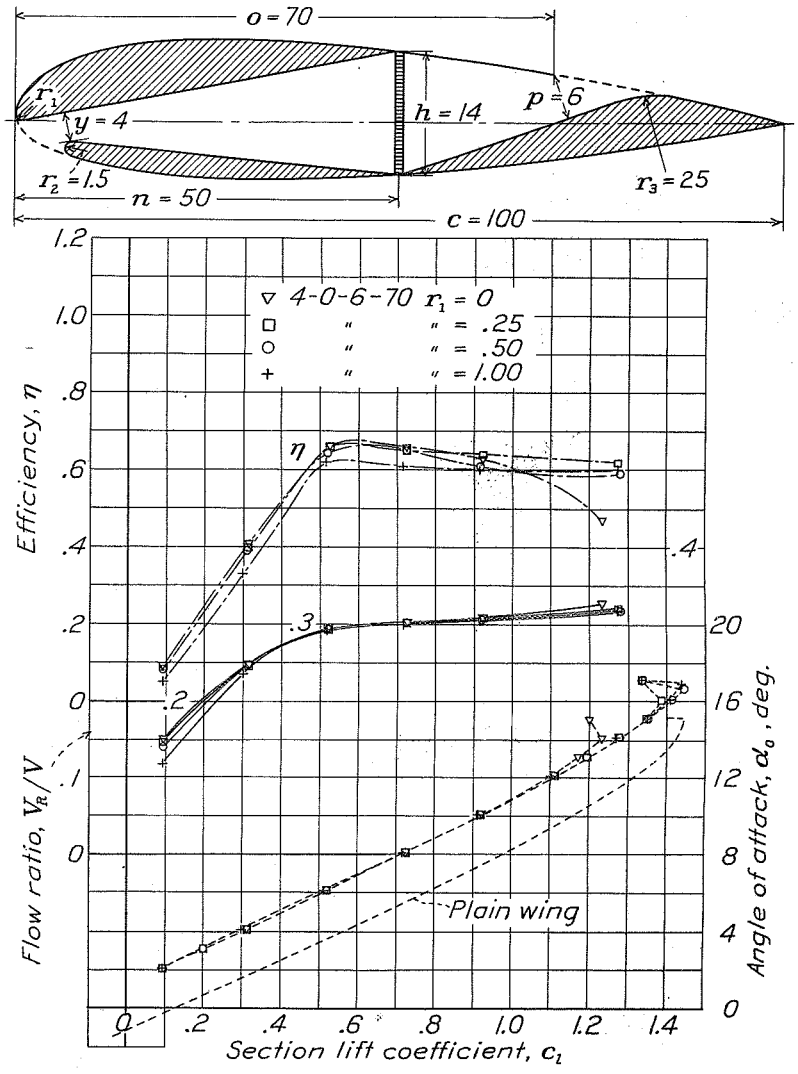

Figure 12 b.

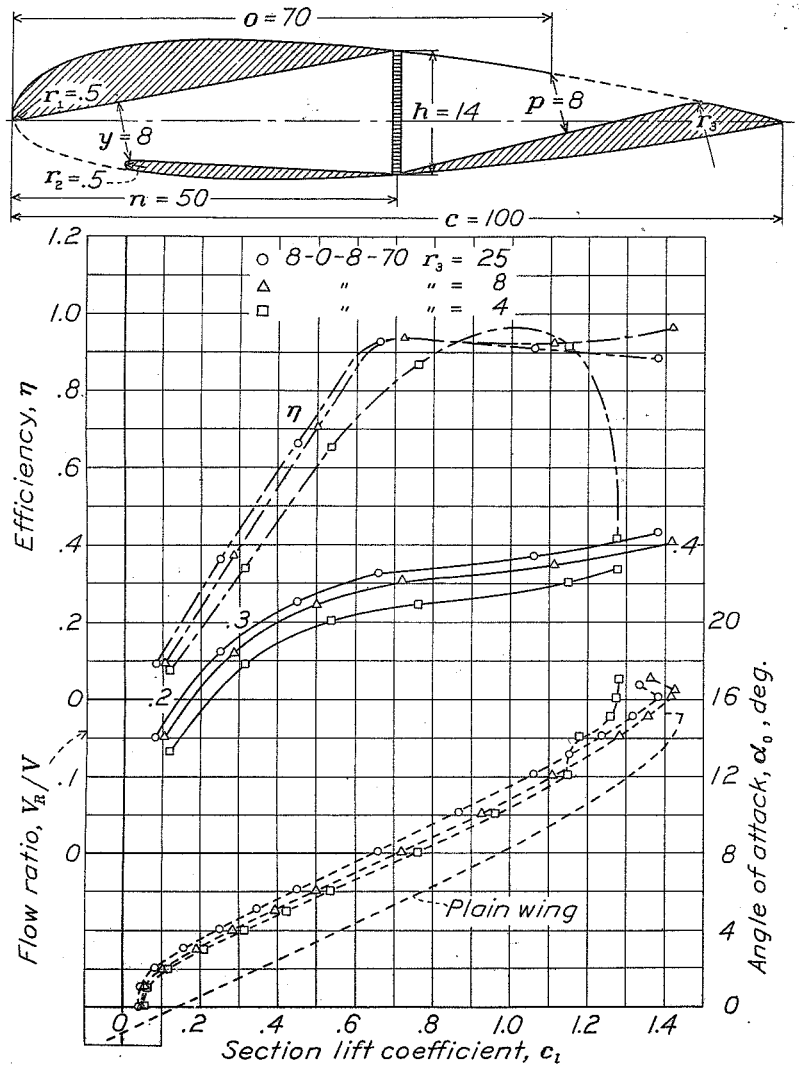

Figure 13a

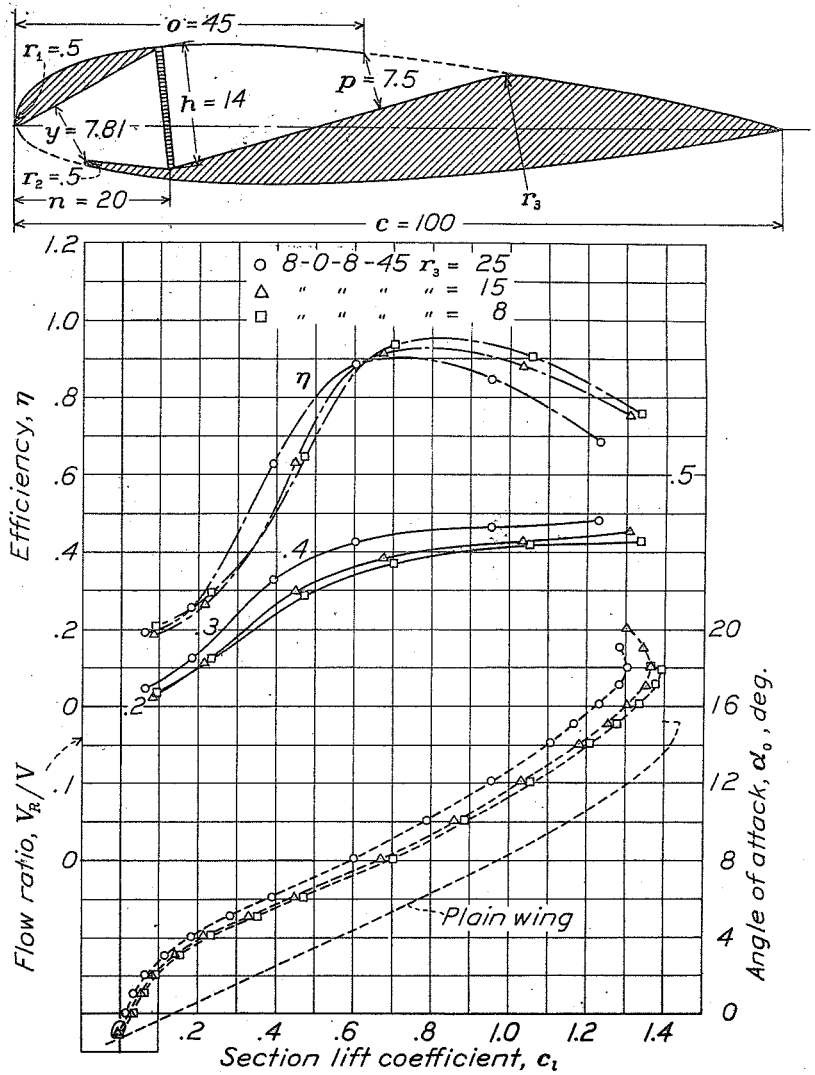

Figure 13b

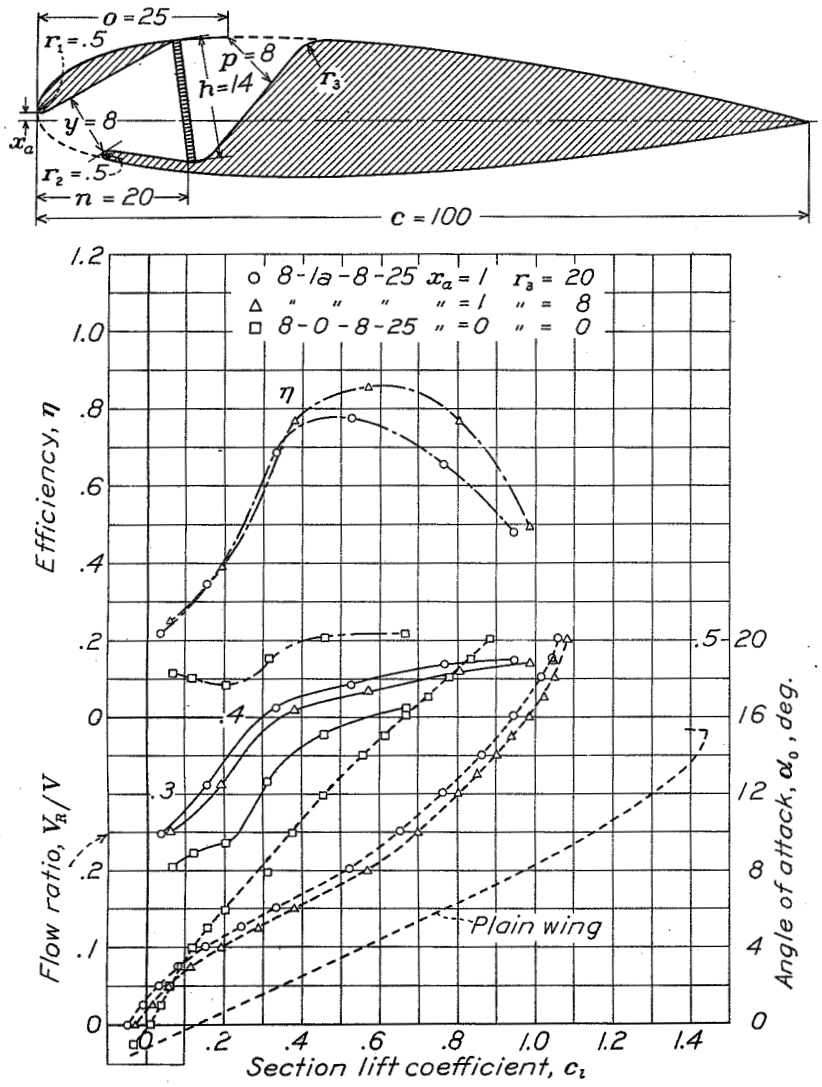

Figure 13c

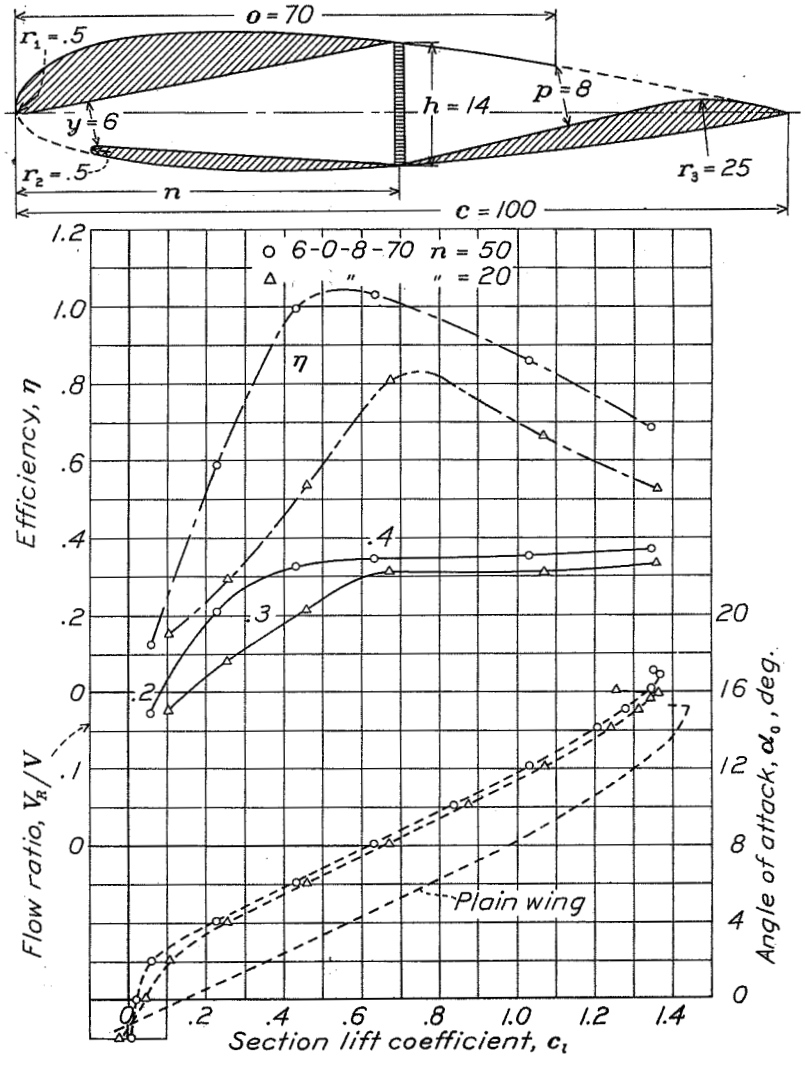

Figure 14.

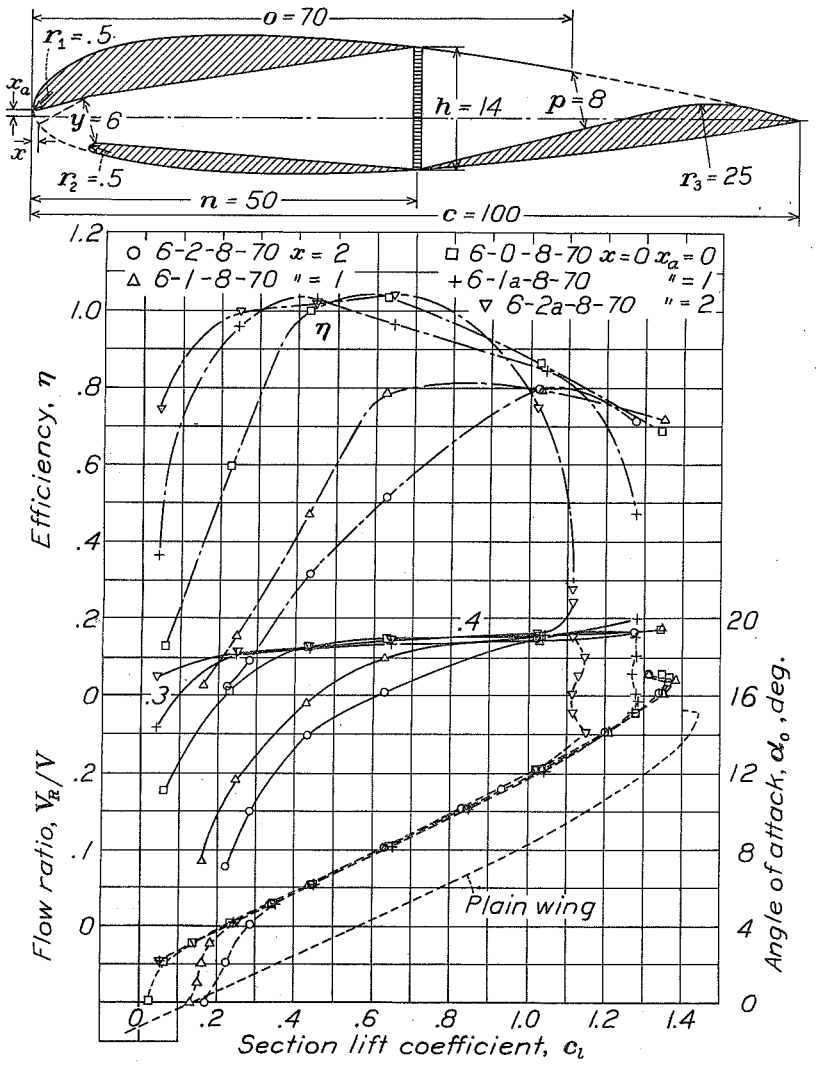

Figure 15 a.

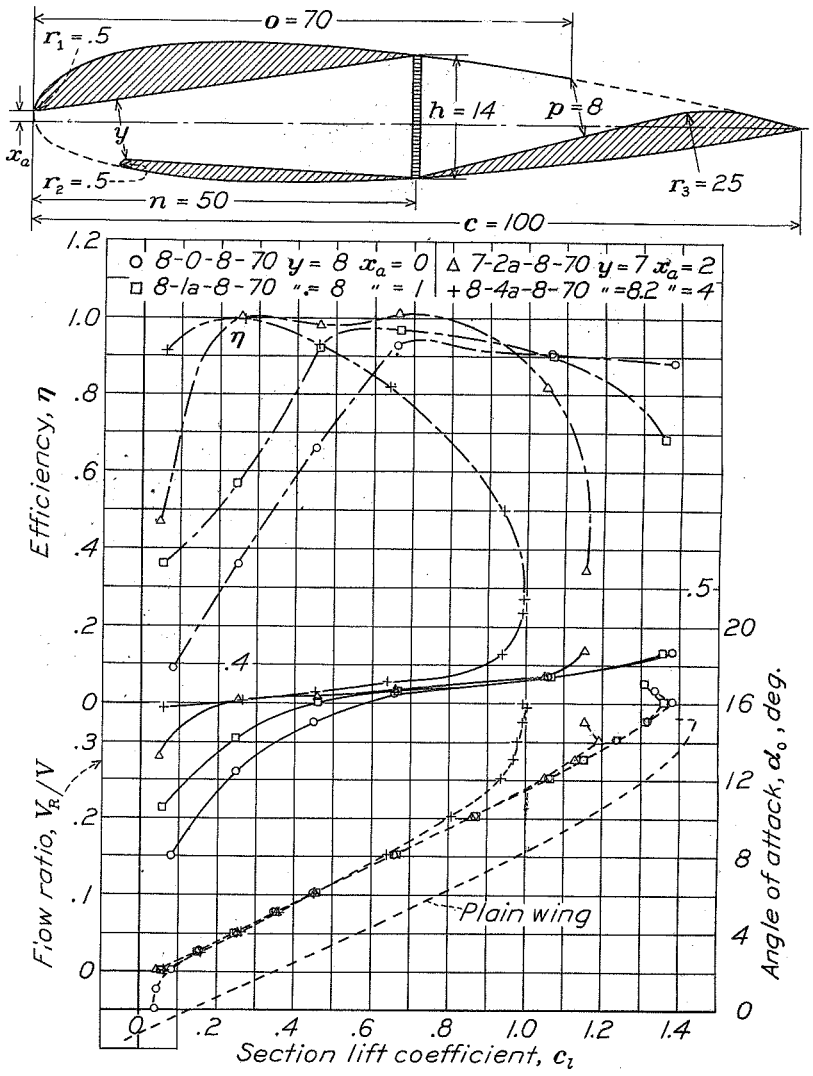

Figure 15 b.

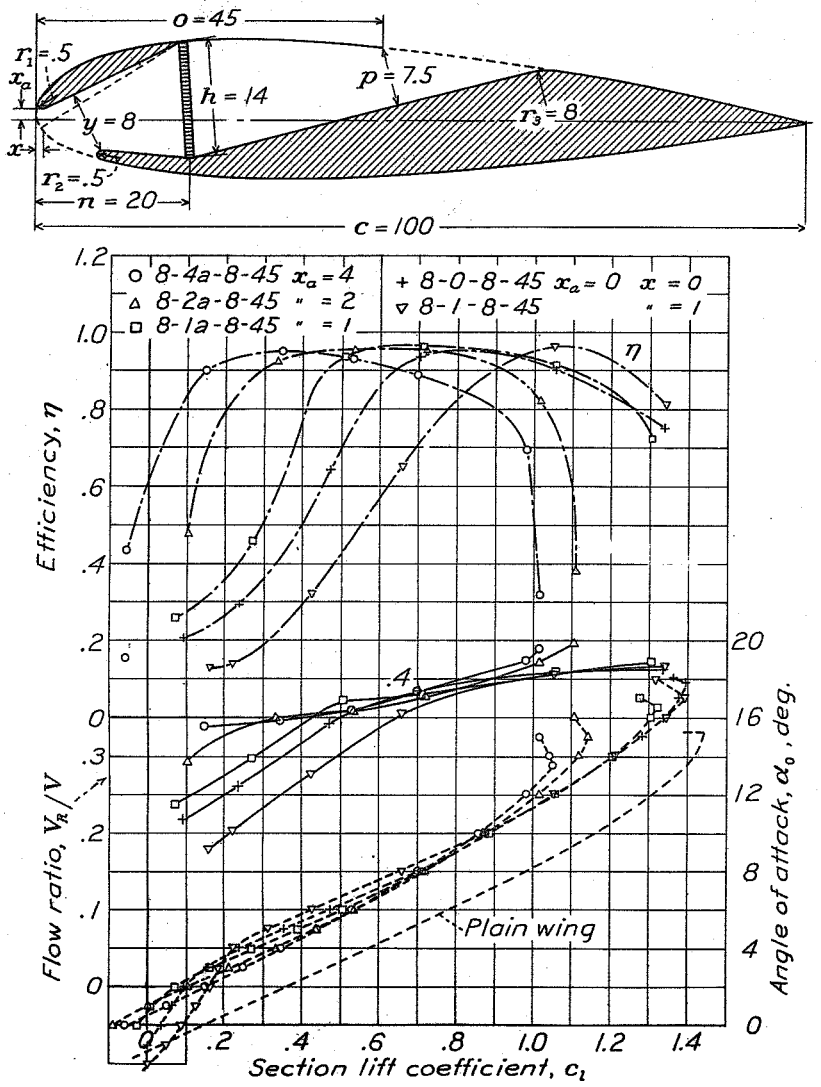

Figure 16

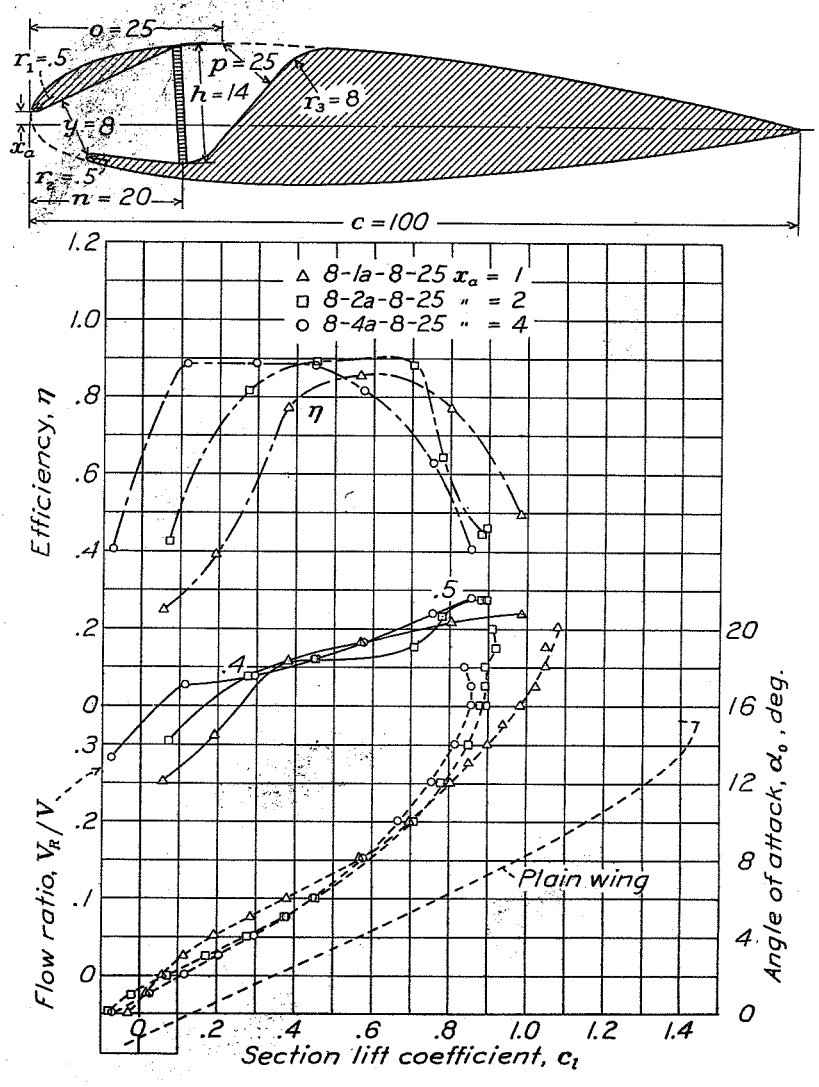

Figure 17a

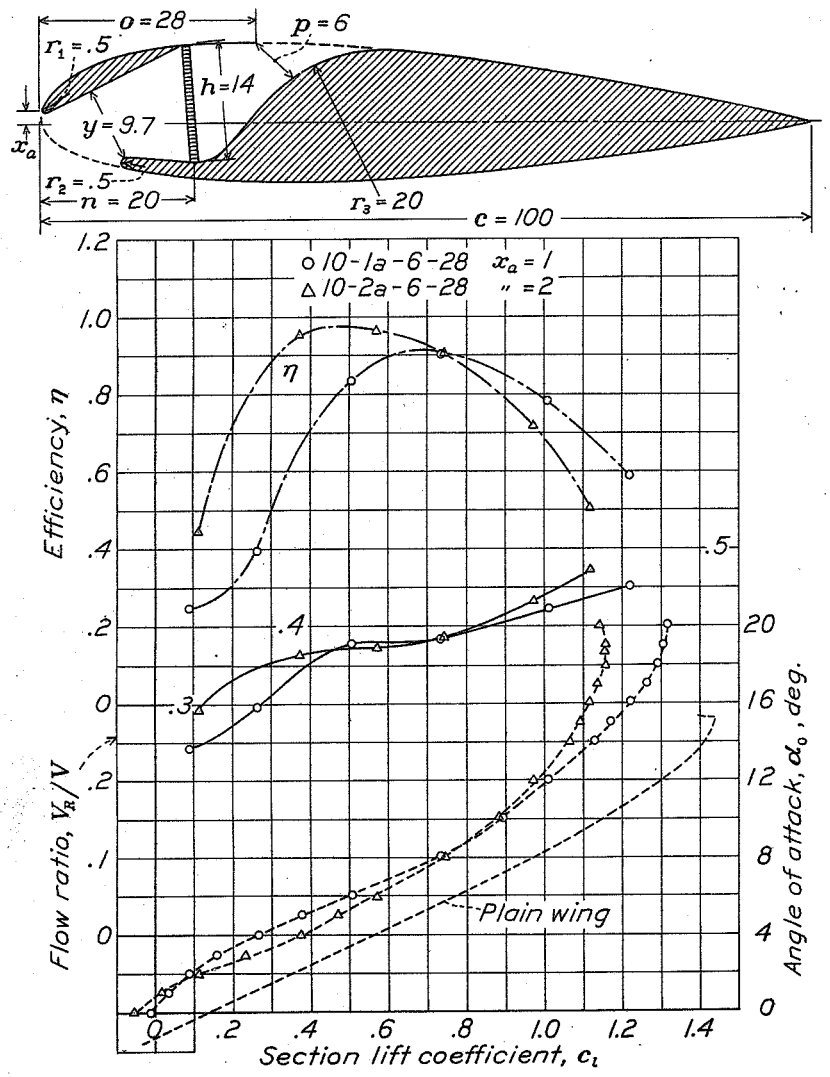

Figure 17b

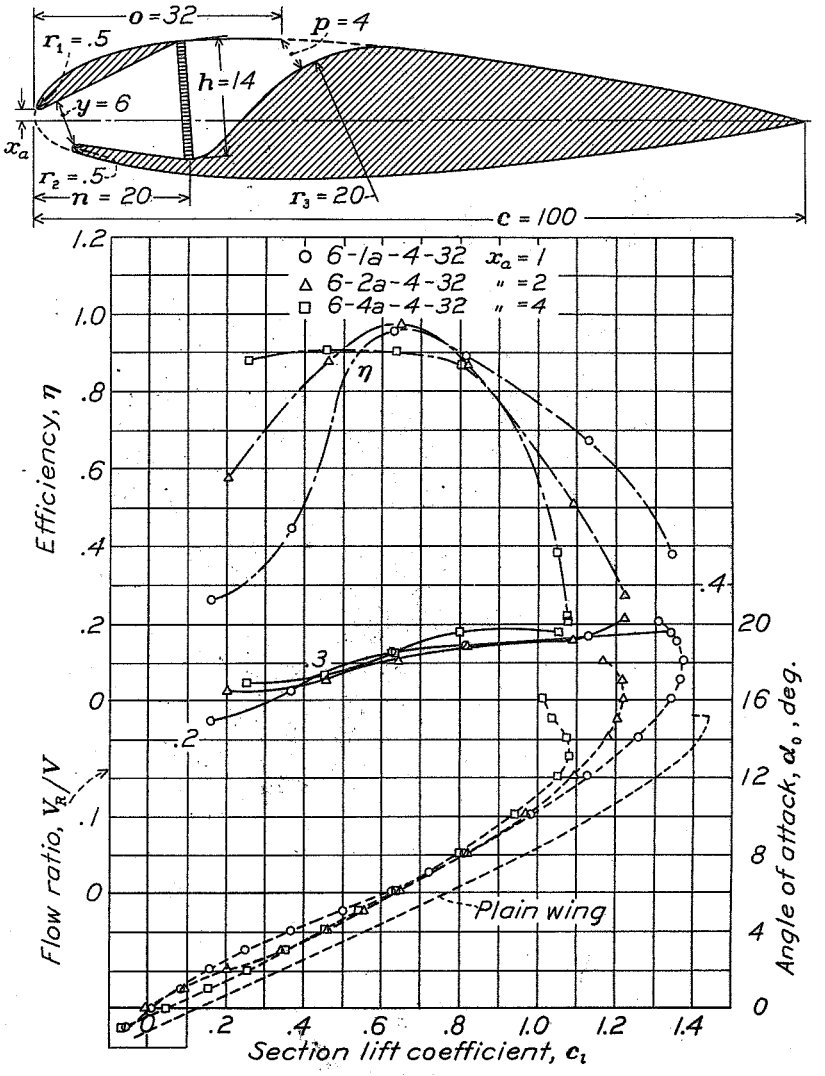

Figure 17c

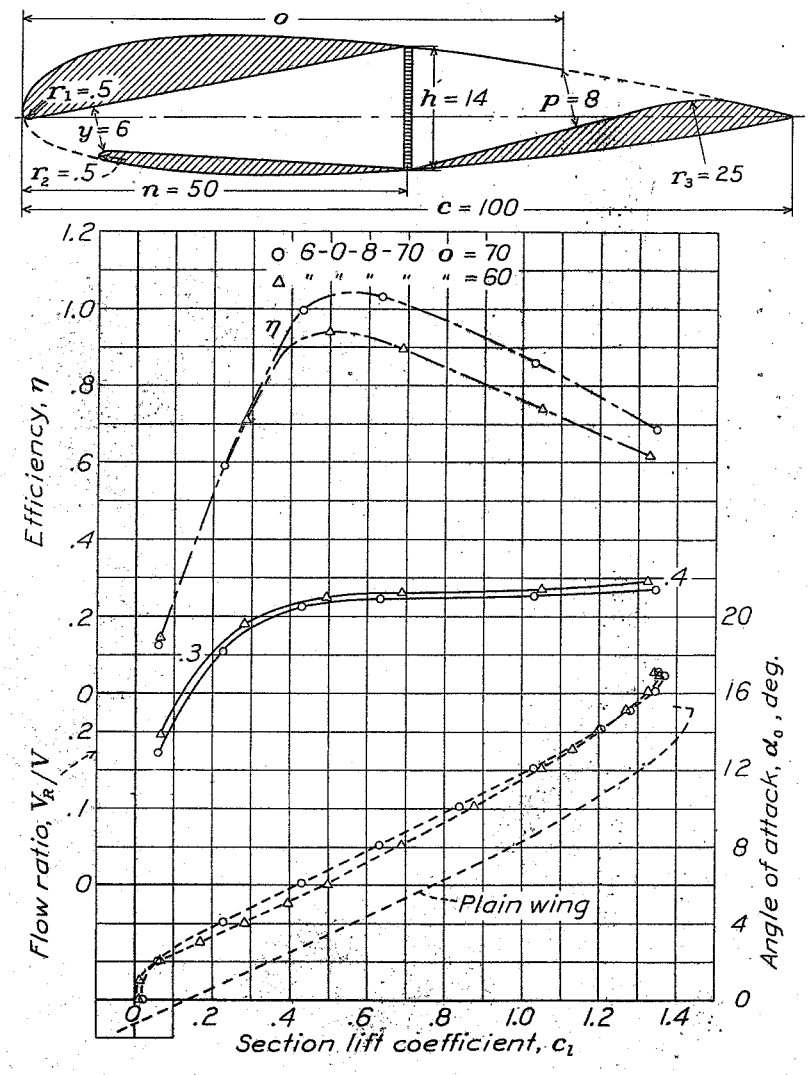

Figure 18a

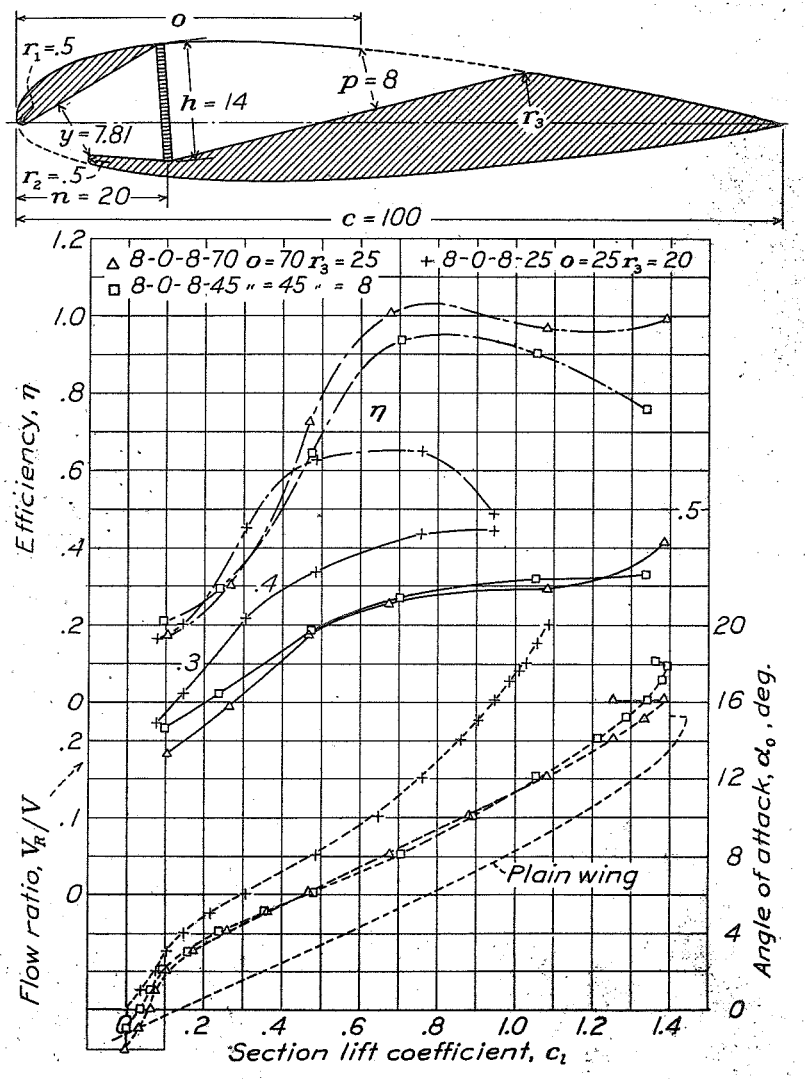

Figure 18b

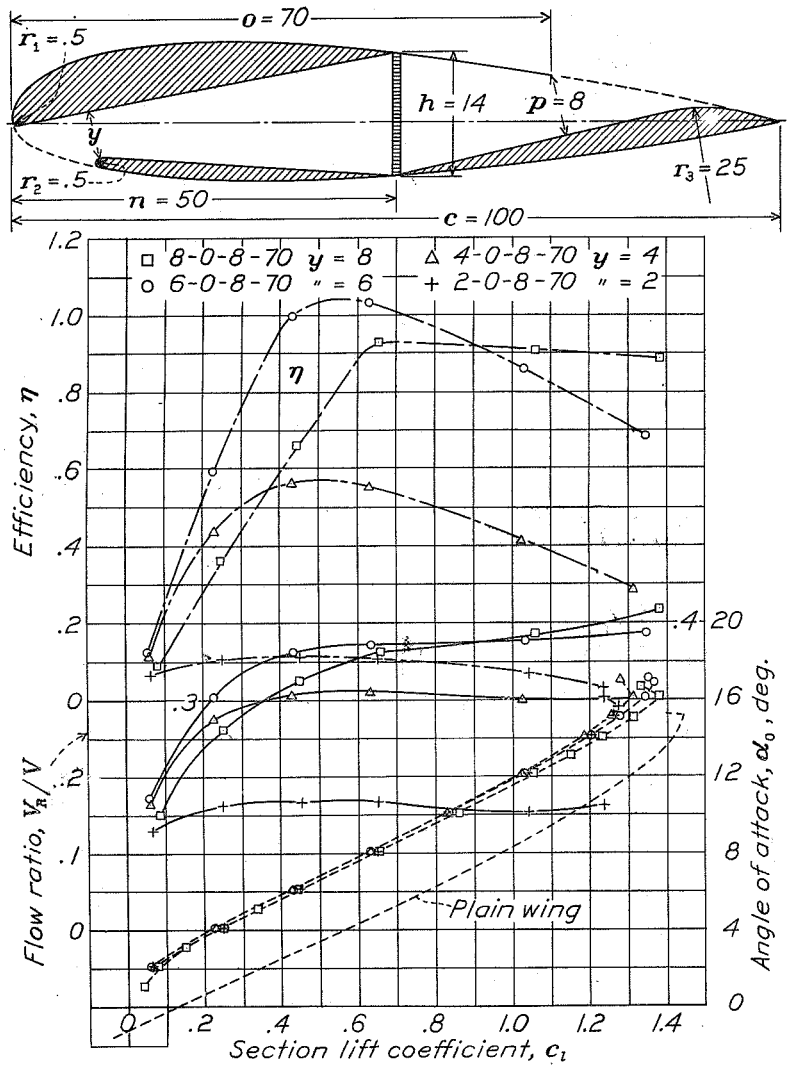

Figure 19 a.

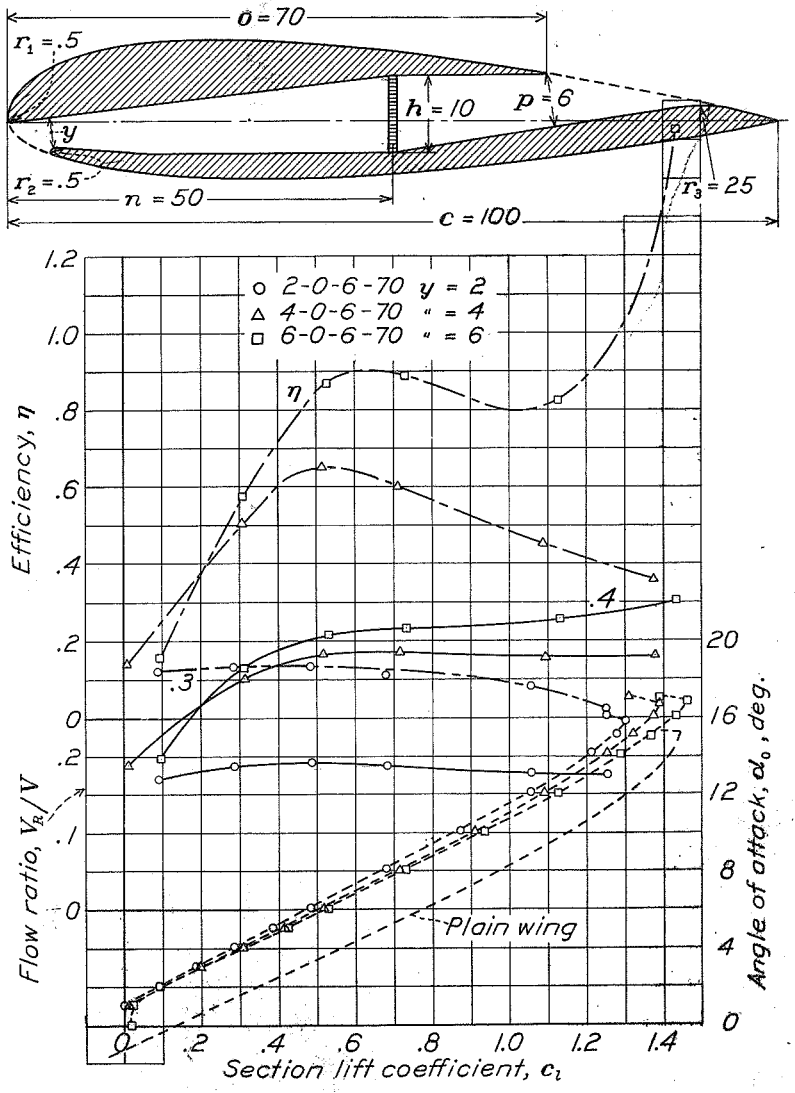

Figure 19 b.

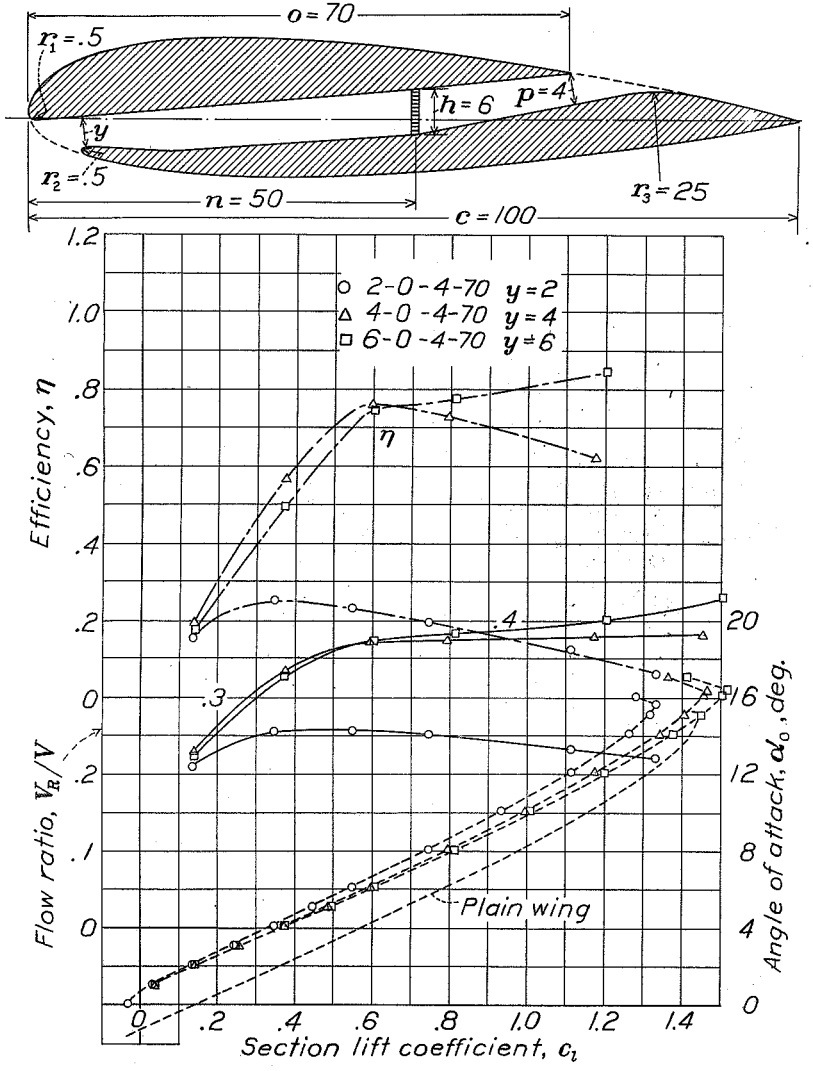

Figure 19 c.

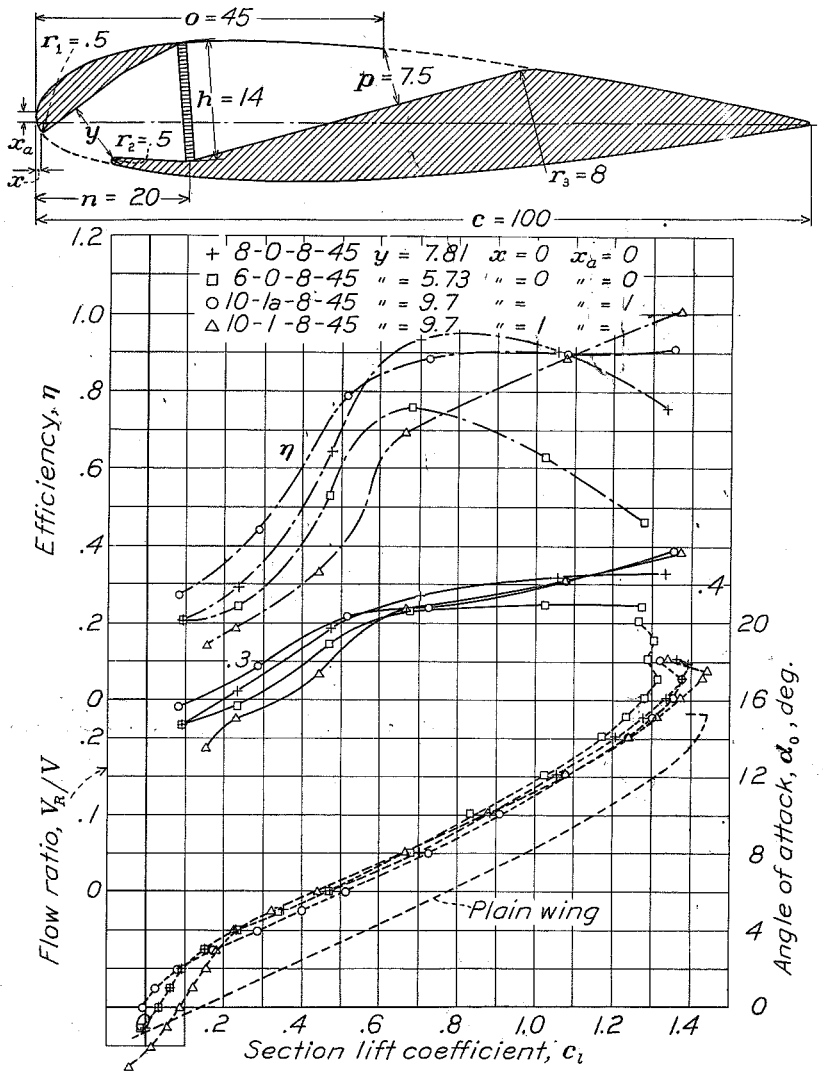

Figure 20.

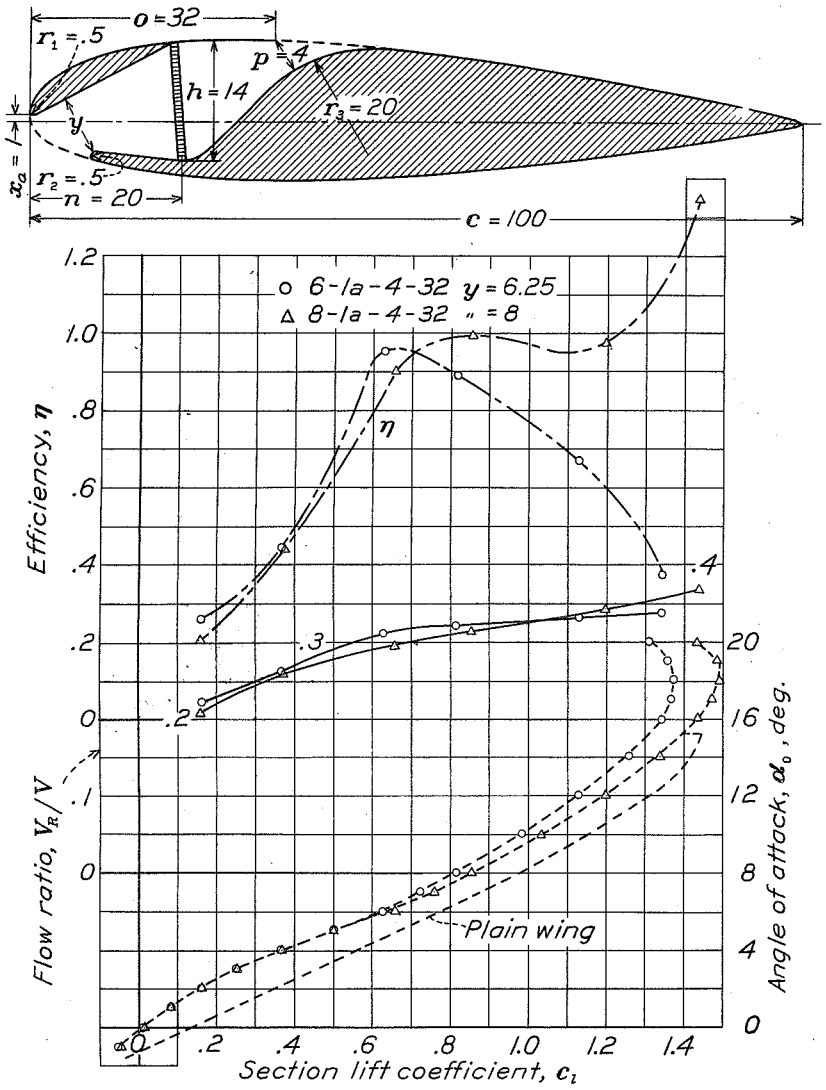

Figure 21 a.

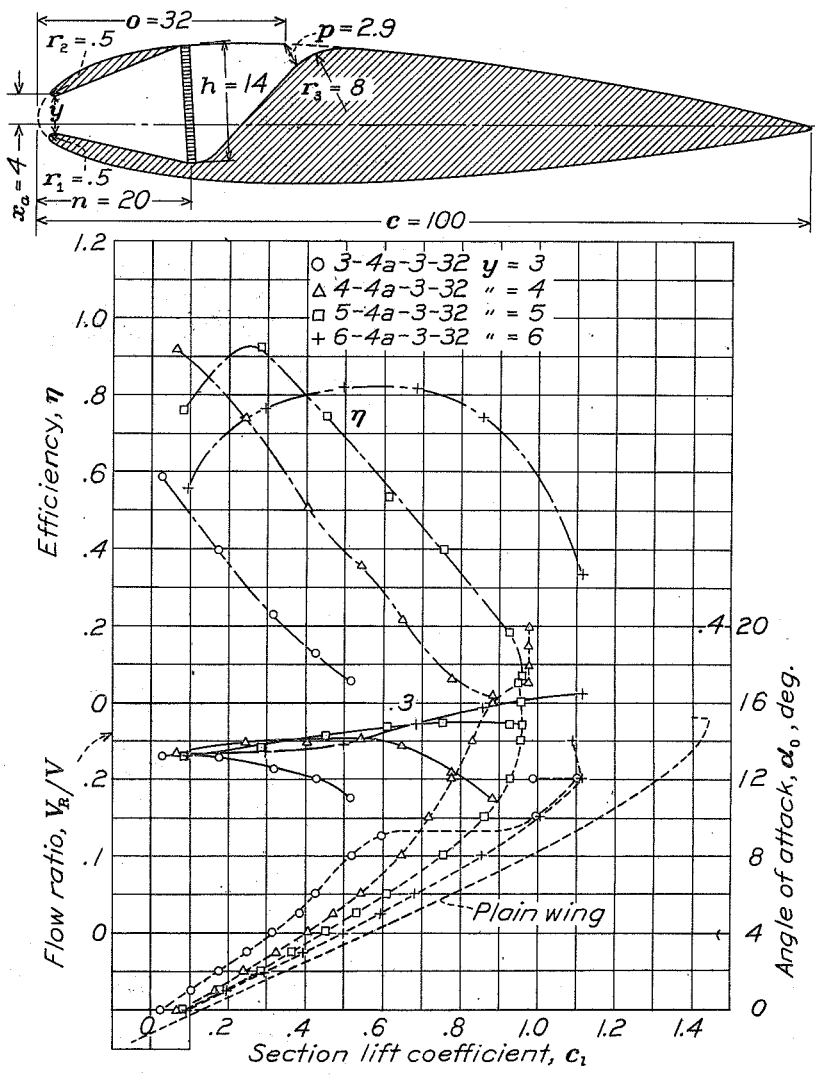

Figure 21 b.

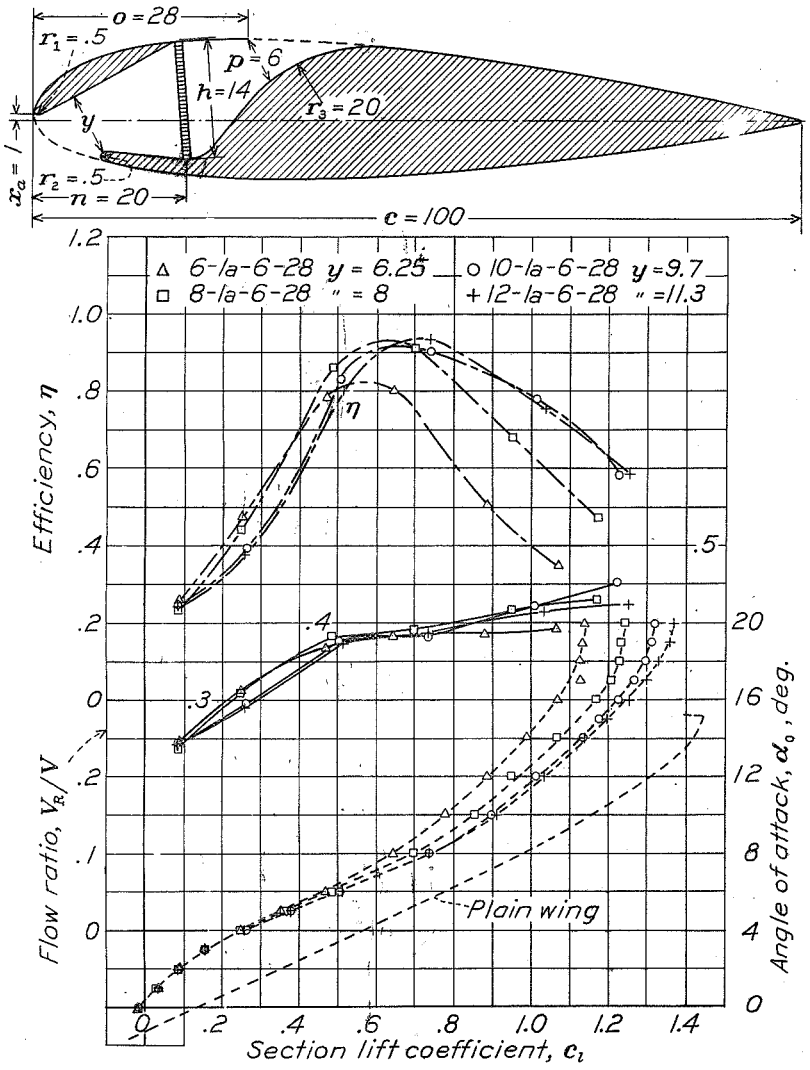

Figure 22 a.

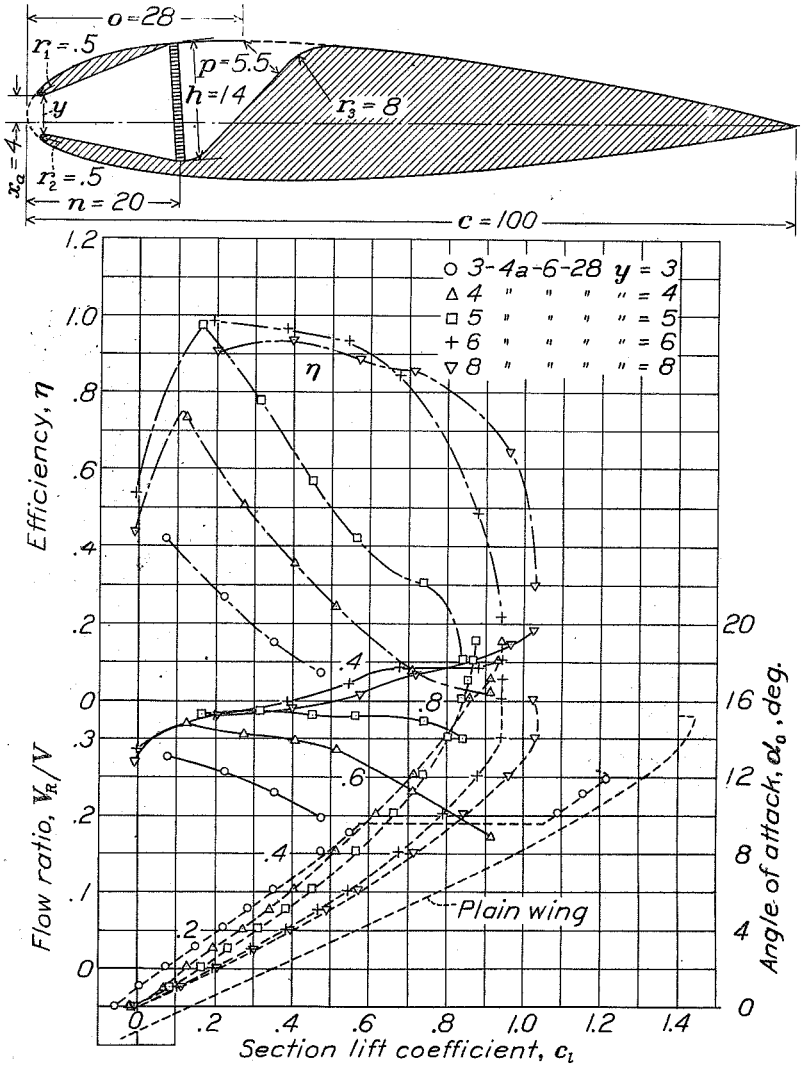

Figure 22 b.

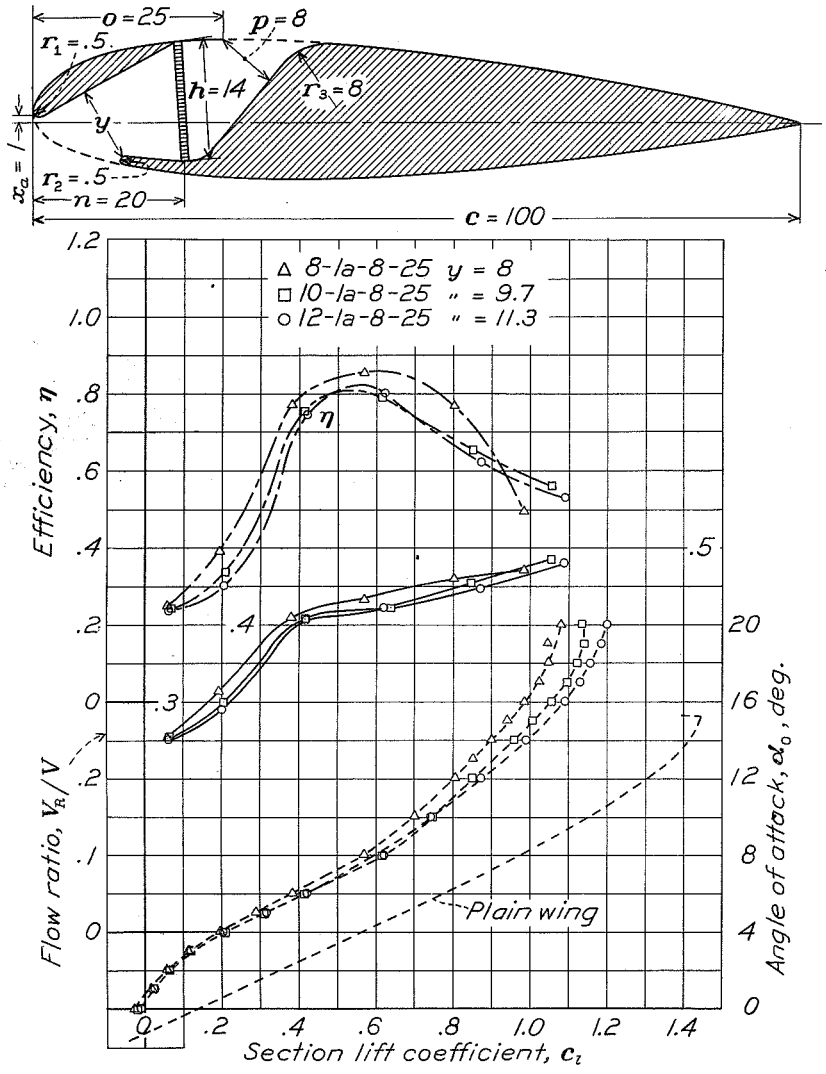

Figure 23 a.

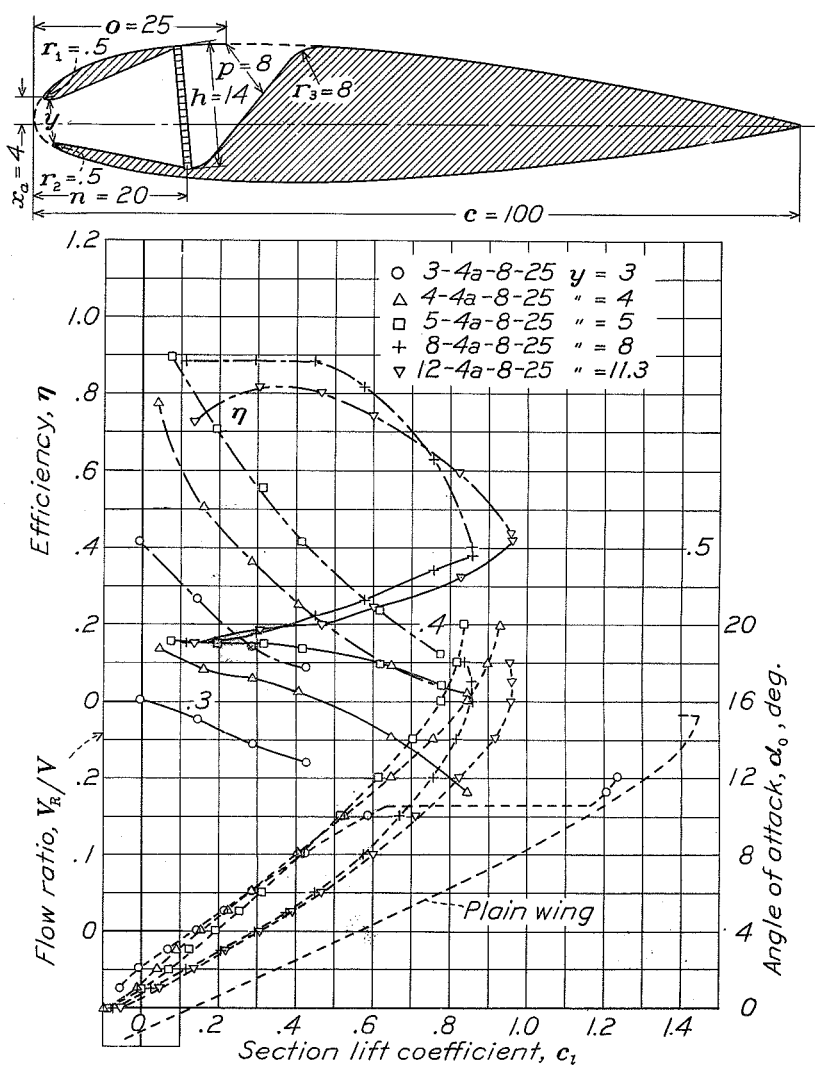

Figure 23 b.

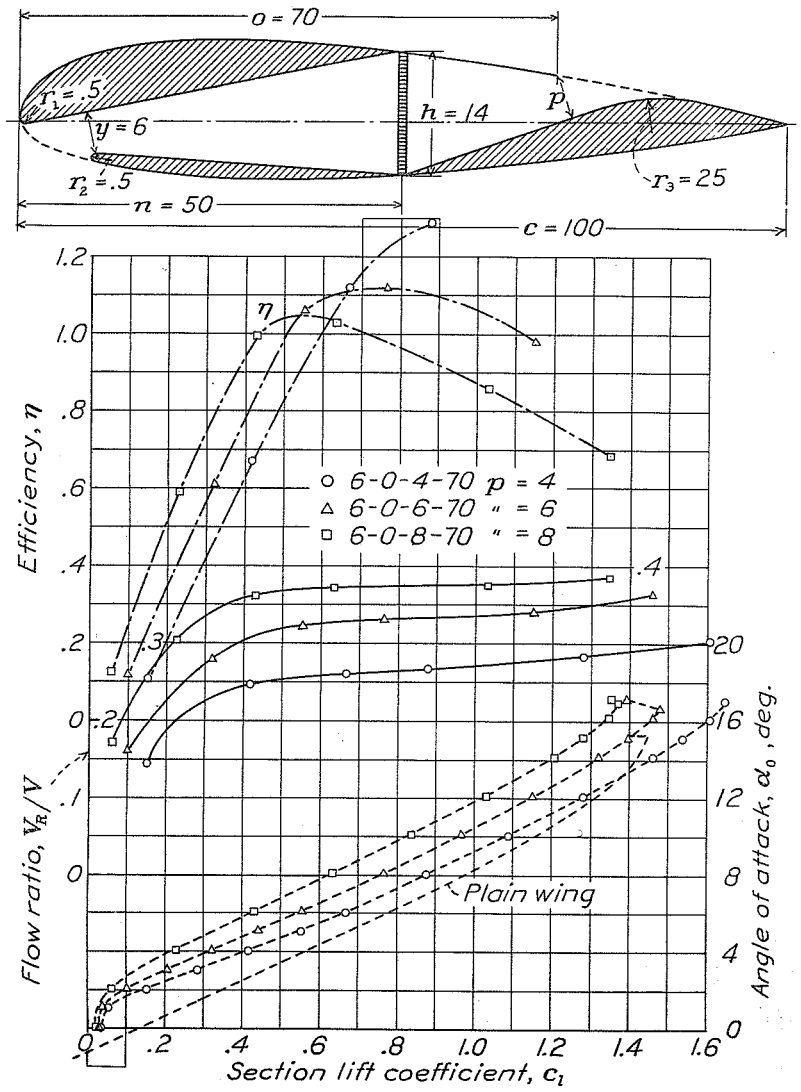

Figure 24a

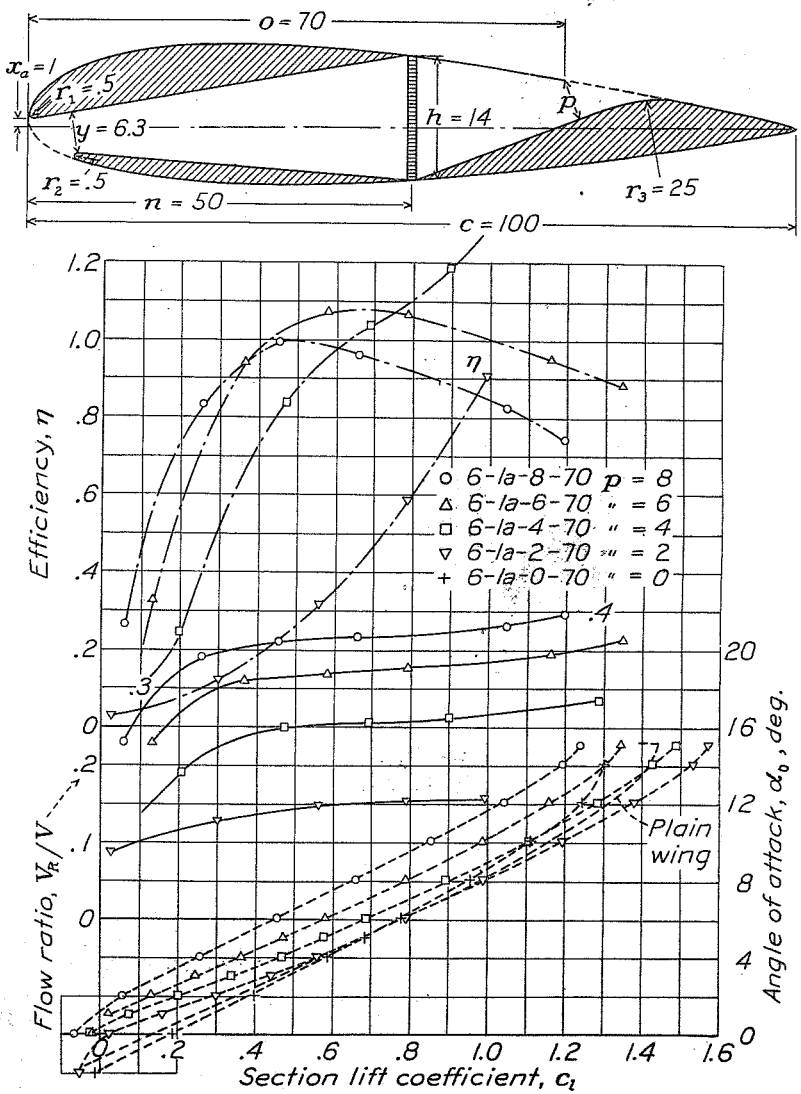

Figure 24b

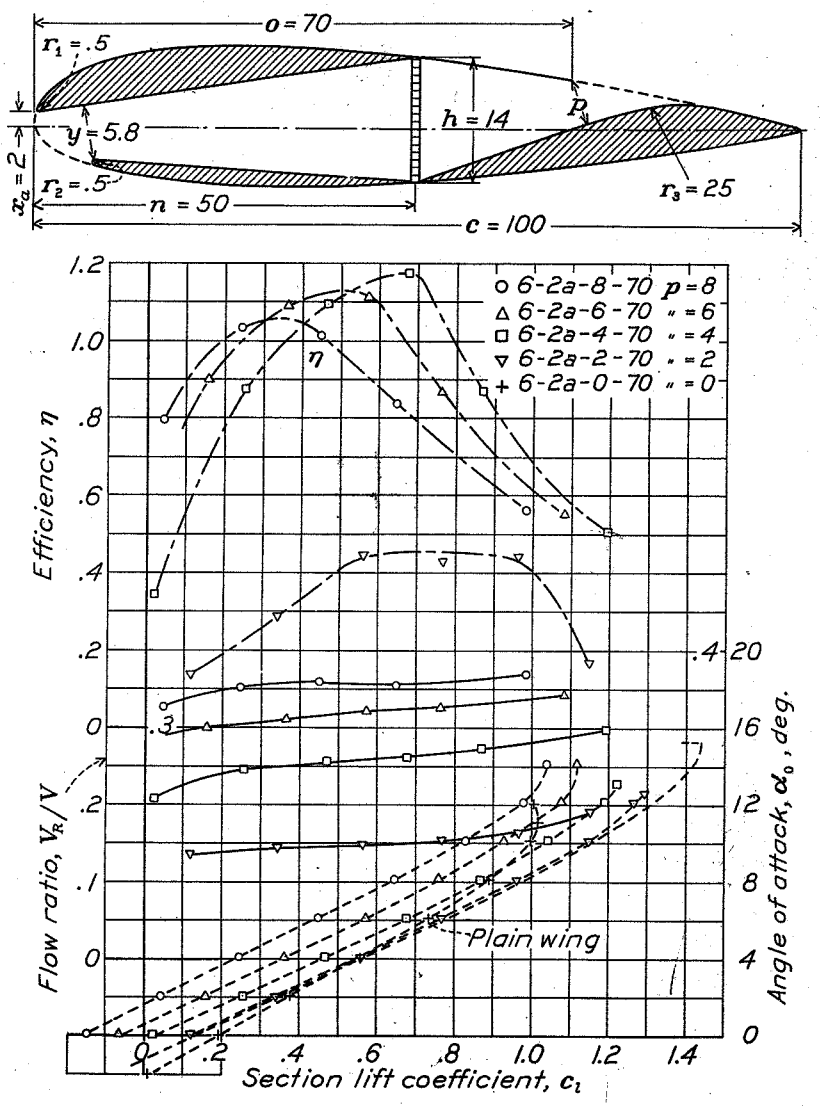

Figure 24c

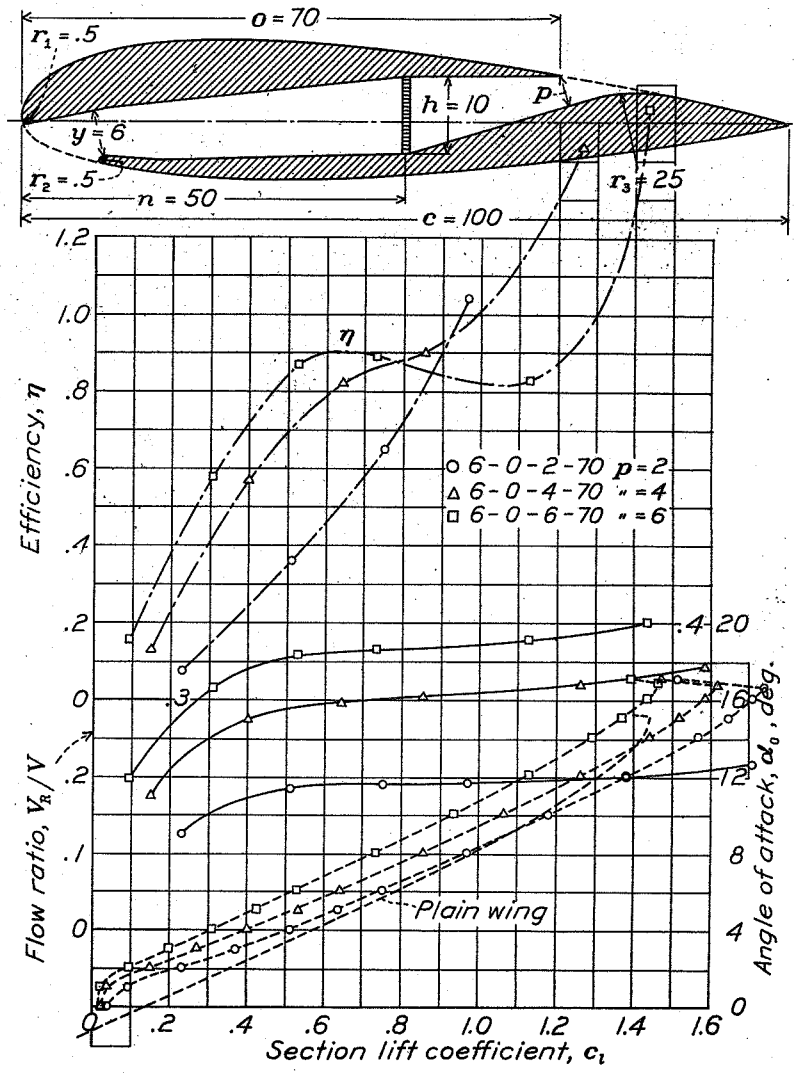

Figure 24d

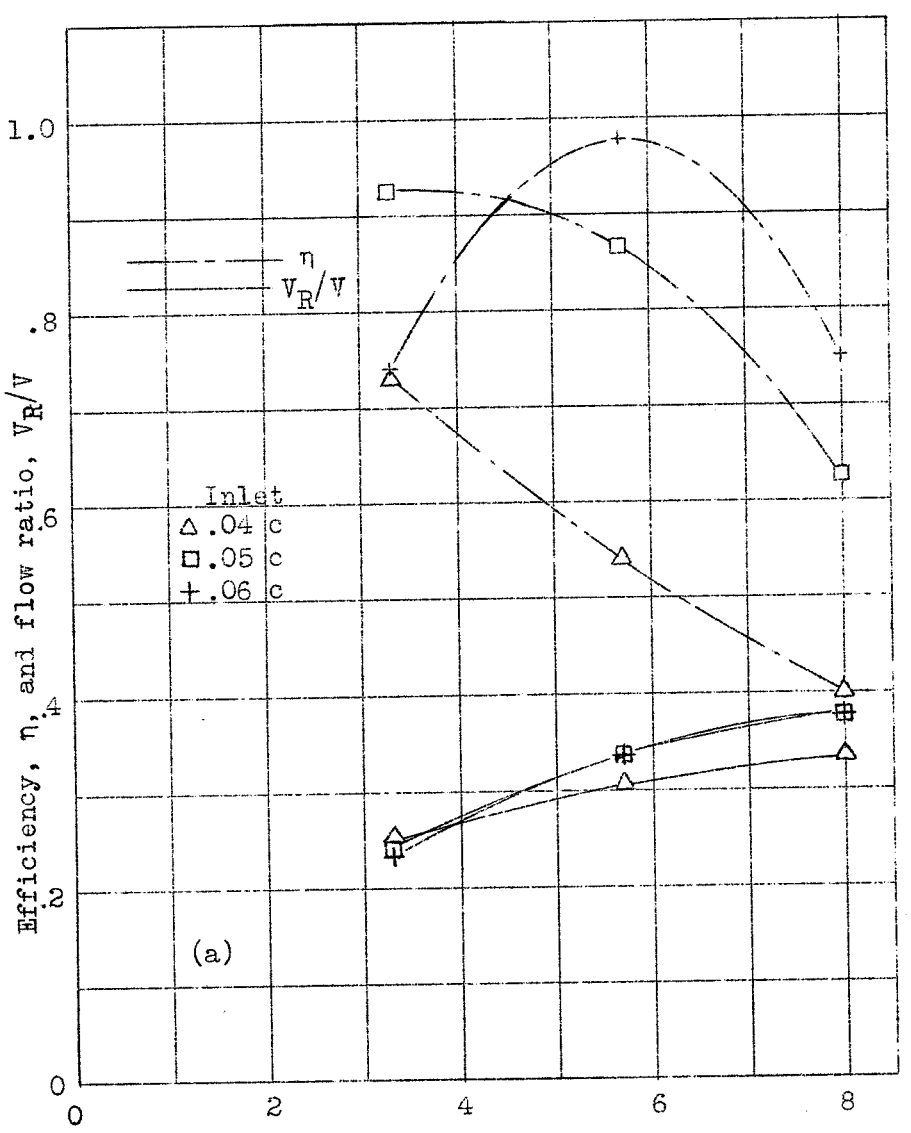

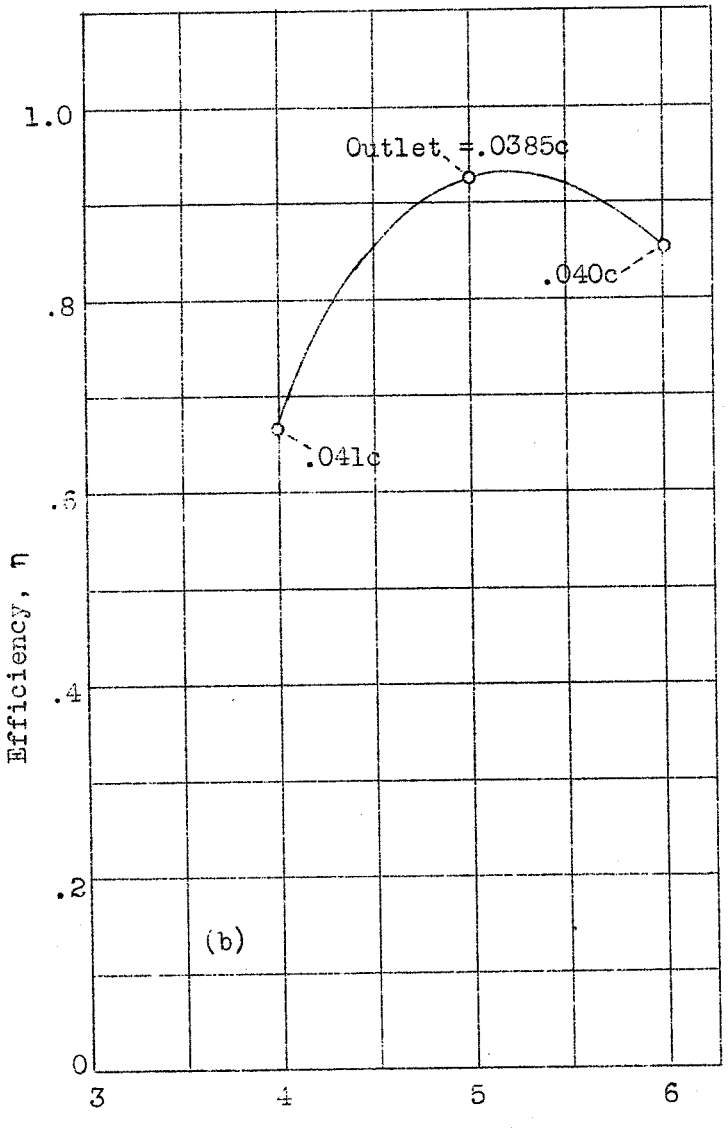

N.A.C.A.

Fig. 25 a,b.

Figure 25 a,b.